A Long-Acting Prostacyclin Agonist with Thromboxane Inhibitory Activity for Pulmonary Hypertension

Masaharu Kataoka, Noritoshi Nagaya, Toru Satoh, Takefumi Itoh, Shinsuke Murakami, Takashi Iwase, Yoshinori Miyahara, Shingo Kyotani, Yoshiki Sakai, Kenji Kangawa, and Satoshi Ogawa

Department of Regenerative Medicine and Tissue Engineering and Department of Biochemistry, National Cardiovascular Center Research Institute; Department of Internal Medicine, National Cardiovascular Center; Ono Pharmaceutical Co., Ltd., Research Headquarters, Osaka; and Cardiopulmonary Division, Department of Medicine, Keio University School of Medicine, Tokyo, Japan

Rationale: The balance between prostacyclin and thromboxane plays an important role in the regulation of pulmonary vascular tone. Recently, we developed ONO-1301, a novel, long-acting prostacyclin agonist with thromboxane synthase inhibitory activity.
Objectives: We investigated whether modulation of prostacyclin/thromboxane balance by ONO-1301 ameliorates monocrotaline-induced pulmonary hypertension in rats.
Methods: After subcutaneous injection of monocrotaline or vehicle, rats were randomized to receive repeated subcutaneous administration of ONO-1301 or vehicle twice per day for 3 wk.
Measurements and Main Results: There was significant development of pulmonary hypertension 3 wk after monocrotaline injection. Treatment with ONO-1301 significantly attenuated the increases in right ventricular systolic pressure and ratio of right ventricular weight to body weight in monocrotaline rats. Furthermore, ONO-1301 significantly attenuated the increase in medial wall thickness of peripheral pulmonary arteries in monocrotaline rats. The half-life of plasma ONO-1301 concentration after a single subcutaneous administration was approximately 5.6 h. A single administration of ONO-1301 increased plasma cyclic adenosine 3′, 5′-monophosphate level, which lasted at least up to 8 h. Treatment with ONO-1301 significantly decreased plasma 11-dehydro-thromboxane B_2, a metabolite of thromboxane, in monocrotaline rats. Finally, Kaplan-Meier survival curves demonstrated that repeated administration of ONO-1301 improved survival rate in monocrotaline rats compared with vehicle administration (80 vs. 30% in 6-wk survival).
Conclusions: Subcutaneous administration of a novel prostacyclin agonist (ONO-1301) markedly attenuated monocrotaline-induced pulmonary hypertension and improved survival in rats. The beneficial effects of ONO-1301 may occur through its long-lasting stimulation of cyclic adenosine 3′, 5′-monophosphate and inhibition of thromboxane synthase.

Keywords: cAMP; monocrotaline; hemodynamics; vascular remodeling

Pulmonary arterial hypertension is a rare but life-threatening disease (1, 2). The pathogenesis includes pulmonary vasoconstriction, endothelial cell proliferation, smooth muscle cell proliferation, and *in situ* thrombosis (3, 4). Prostacyclin, a metabolite of arachidonic acid, has vasoprotective effects, including vasodilation, antiplatelet aggregation, and inhibition of smooth muscle cell proliferation (5–8). Thus, continuous intravenous infusion of prostacyclin (epoprostenol) has become recognized as a therapeutic breakthrough for pulmonary arterial hypertension (9–16). The dramatic success of long-term intravenous prostacyclin has led to the development of prostacyclin analogs (oral beraprost, aerosolized iloprost, and subcutaneous treprostinil; Figure 1) (17–20). Nevertheless, treatment with prostacyclin or its analogs has some problems in the clinical setting. Their duration of acting is so short that they need to be continuously infused or frequently administered (9–20). In addition, these compounds failed to inhibit thromboxane synthesis during treatment (21).

We developed a new type of prostacyclin agonist, ONO-1301, which has long-lasting prostacyclin activity and thromboxane synthase inhibitory activity. Prostacyclin and its analogs are unstable because 15-hydroxyprostaglandin dehydrogenase metabolizes their prostanoid structures, including a five-membered ring and allylic alcohol. In contrast, ONO-1301 is chemically and biologically stable because of the absence of prostanoid structures. Interestingly, ONO-1301 has thromboxane synthase inhibitory activity because of the presence of a 3-pyridine radical. It has been reported that augmented release of thromboxane A_2, which is both a potent pulmonary vasoconstrictor and a procoagulant (22), occurs in patients with pulmonary hypertension (23, 24). The imbalance of thromboxane and prostacyclin is considered to contribute to the development of pulmonary arterial hypertension. These findings raise the possibility that administration of ONO-1301 may have beneficial effects on pulmonary hemodynamics.

Thus, the purposes of this study were (*1*) to investigate whether a single subcutaneous administration of ONO-1301 has long-lasting prostacyclin activity in rats, (*2*) to investigate whether subcutaneous administration of ONO-1301 inhibits thromboxane synthesis in monocrotaline (MCT)-induced pulmonary hypertension in rats, (*3*) to examine whether intermittent subcutaneous ONO-1301 improves pulmonary hemodynamics and survival in MCT rats, and (*4*) to elucidate the underlying mechanisms responsible for the beneficial effects of this compound.

METHODS

Animals

We used 95 male Wistar rats weighing 100 to 120 g. The rats were randomly given a subcutaneous injection of either 60 mg/kg MCT (MCT rats) or 0.9% saline (vehicle) and assigned to receive repeated subcutaneous injection of ONO-1301 (Ono Pharmaceutical Co., Ltd., Osaka, Japan) or vehicle. This protocol resulted in the creation of three groups: sham rats given vehicle (n = 10), MCT rats given vehicle (n = 10), and MCT rats treated with ONO-1301 (n = 13). In addition, 20 rats were studied to evaluate the effect of ONO-1301 on survival in MCT rats. Furthermore, 42 rats were studied to evaluate the effect of ONO-1301 on plasma cAMP level (n = 12) and 11-dehydro-thromboxane B_2 (TXB_2) level (n = 30).

In Vivo Experimental Protocol

After rats were anesthetized by intraperitoneal injection of pentobarbital (30 mg/kg), they were given a subcutaneous injection of either

(Received in original form January 22, 2005; accepted in final form September 23, 2005)

Supported by grants from Ono Pharmaceutical Co., Ltd.

Correspondence and requests for reprints should be addressed to Noritoshi Nagaya, M.D., Department of Regenerative Medicine and Tissue Engineering, National Cardiovascular Center Research Institute, 5-7-1 Fujishirodai, Suita, Osaka 565-8565, Japan. E-mail: nnagaya@ri.ncvc.go.jp

Am J Respir Crit Care Med Vol 172. pp 1575–1580, 2005
Originally Published in Press as DOI: 10.1164/rccm.200501-102OC on September 28, 2005
Internet address: www.atsjournals.org

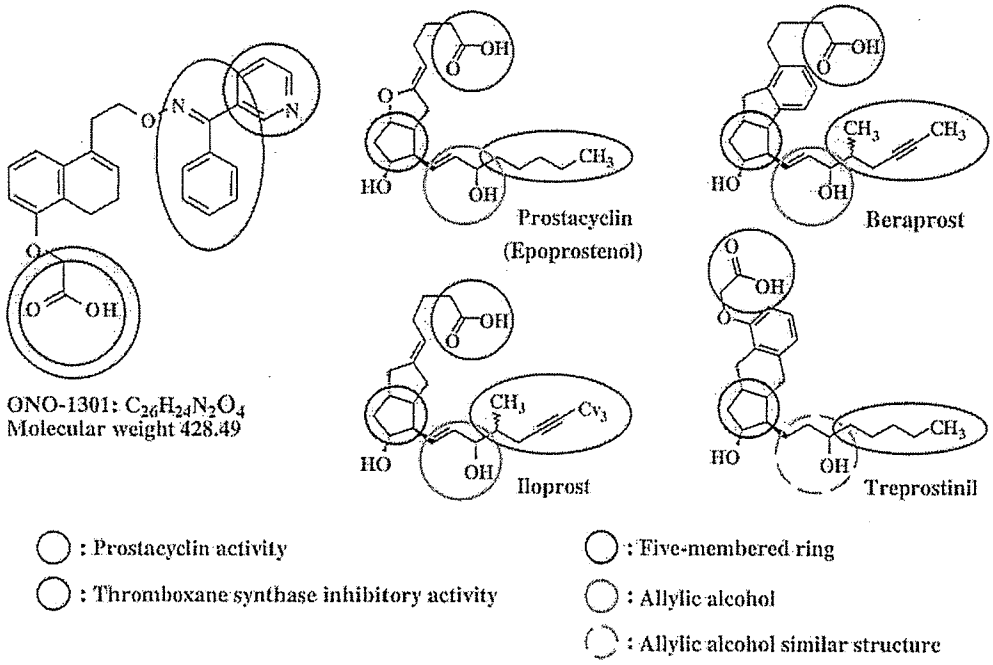

Figure 1. Molecular structures of ONO-1301, epoprostenol, and conventional prostacyclin analogs (beraprost, iloprost, and treprostinil). Epoprostenol and prostacyclin analogs share common characteristic prostanoid structures, including a five-membered ring and allylic alcohol (*blue and yellow circles*). In contrast, ONO-1301 has a carboxylic acid and a lipid-soluble functional group that activate the prostacyclin receptor (*green circles*), but does not have prostanoid structures, which allows long-lasting prostacyclin activity. Unlike epoprostenol and conventional prostacyclin analogs, ONO-1301 has thromboxane synthase inhibitory activity because of a 3-pyridine radical and carboxylic acid within its molecule (*red circles*).

60 mg/kg MCT or vehicle. Then, ONO-1301 (20 mg/kg/d) or vehicle was injected subcutaneously twice per day for 3 wk after MCT injection. Animals were maintained on standard rat chow. Hemodynamic studies were performed on Day 22. A polyethylene catheter (PE-50) was inserted into the right carotid artery to measure heart rate and mean arterial pressure. A polyethylene catheter (PE-50) was inserted through the right jugular vein into the right ventricle (RV) for measurement of RV pressure. Finally, cardiac arrest was induced by injection of 2 mmol/L potassium chloride through the catheter. The ventricles and lungs were excised, dissected free, and weighed. The ratio of RV weight to body weight (RV/BW), the ratio of left ventricular plus septal weight to body weight (LV + S/BW), and the ratio of RV weight to left ventricular plus septal weight (RV/LV + S) were calculated as indexes of ventricular hypertrophy, as reported previously (25). All protocols were performed in accordance with guidelines of the Animal Care Ethics Committee of the National Cardiovascular Center Research Institute.

Morphometric Analysis of Pulmonary Arteries

Paraffin sections 4-μm thick were obtained from the middle region of the right lung and stained with elastic van Gieson for examination by light microscopy. The external diameter and medial wall thickness of the pulmonary arteries were measured in 20 muscular arteries (ranging in size from 25 to 100 μm in external diameter) by two investigators who were blinded to treatment allocation. For each artery, the medial wall thickness was expressed as follows: % wall thickness = ([medial thickness × 2]/external diameter) × 100, as reported previously (26).

Assay for Plasma ONO-1301 Concentration

To estimate the half-life of ONO-1301, we measured plasma ONO-1301 concentration in rats after a subcutaneous injection (n = 4). Blood was drawn at 0.25, 0.5, 1, 2, 4, 8, and 24 h after a single subcutaneous administration of ONO-1301 (10 mg/kg). Plasma ONO-1301 concentration was measured by liquid chromatography tandem mass spectrometry assay.

Assay for Plasma cAMP Level

To investigate whether a single subcutaneous administration of ONO-1301 has long-lasting prostacyclin activity in rats, we measured plasma cAMP levels after ONO-1301 injection. Twelve rats were assigned to receive a single subcutaneous injection of ONO-1301 (10 mg/kg) or vehicle (n = 6 each). Blood was drawn from the right carotid artery at baseline and 1, 2, 4, 6, and 8 h after ONO-1301 injection. Blood was immediately transferred into a chilled glass tube containing disodium ethylenediaminetetraacetic acid (1 mg/ml) and aprotinin (500 U/ml) and centrifuged immediately. Plasma cAMP levels was measured with a radioimmunoassay kit (cAMP assay kit; Yamasa Shoyu, Chiba, Japan), as reported previously (27).

Assay for Plasma 11-dehydro-TXB_2 Level

To investigate the acute effect of ONO-1301 or prostacyclin (epoprostenol) on thromboxane synthesis in MCT rats, we measured plasma 11-dehydro-TXB_2, a metabolite of thromboxane A_2, after administration of ONO-1301 (10 mg/kg), epoprostenol, or vehicle (n = 5 each). Epoprostenol was infused via a polyethylene catheter (PE-50) inserted into the right jugular vein. Infusion of epoprostenol was begun at 10 ng/kg/min, increased gradually to 150 ng/kg/min over 30 min, escalated to 300 ng/kg/min over the next 30 min, and held at this dose for 1 h, as reported previously (21, 28, 29).

To investigate the chronic effect of ONO-1301 on thromboxane synthesis in MCT rats, we measured plasma 11-dehydro-TXB_2 after repeated subcutaneous injection of ONO-1301 (20 mg/kg/d) or vehicle twice per day for 3 wk (n = 5 each). Blood was drawn from the right carotid artery and plasma 11-dehydro-TXB_2 level was measured with an enzyme immunoassay kit (11-dehydro-TXB_2 assay kit; Cayman Chemical Co., Ann Arbor, MI), as reported previously (30).

Survival Analysis

To evaluate the effect of intermittent subcutaneous administration of ONO-1301 on survival in MCT rats, 20 rats received repeated injection of ONO-1301 or vehicle twice per day (n = 10 each). Survival was estimated from the date of MCT injection to the death of the rat or 6 wk after injection.

Statistical Analysis

All data were expressed as mean ± SEM. Comparisons of parameters among the three groups were made by one-way analysis of variance, followed by Newman-Keuls' test. Comparisons of the time course of parameters between the two groups were made by two-way analysis of variance for repeated measures, followed by Newman-Keuls' test. Survival curves were derived by the Kaplan-Meier method and compared by log-rank test. A value of $p < 0.05$ was considered statistically significant.

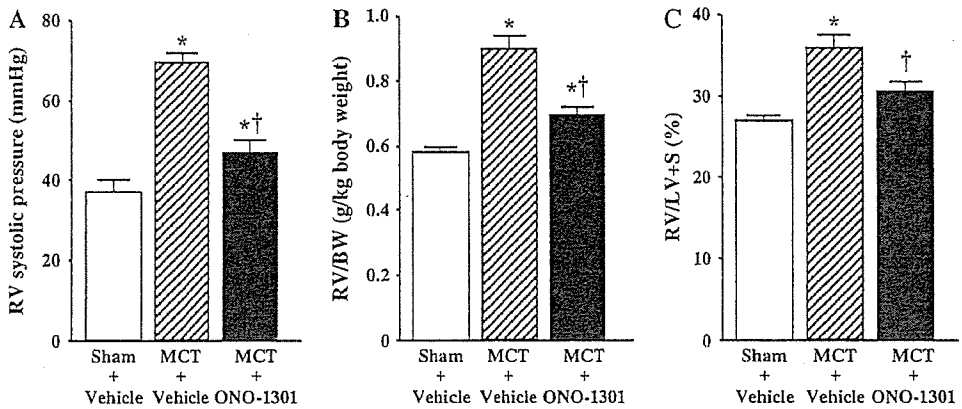

Figure 2. Effects of ONO-1301 on right ventricular (RV) systolic pressure (*A*), RV weight to body weight (RV/BW; *B*), and RV weight to left ventricular plus septal weight (RV/LV + S; *C*) in sham rats given vehicle (sham + vehicle), monocrotaline (MCT) rats given vehicle (MCT + vehicle), and MCT rats treated with ONO-1301 (MCT + ONO-1301). Data are mean ± SEM. *$p < 0.05$ versus sham + vehicle; †$p < 0.05$ versus MCT + vehicle.

RESULTS

Effects of ONO-1301 on Pulmonary Hemodynamics and Vascular Remodeling

RV systolic pressure was significantly increased 3 wk after MCT injection (Figure 2A). However, the increase was significantly attenuated by subcutaneous administration of ONO-1301 (10 mg/kg twice per day). Similarly, the increases in RV/BW and RV/LV + S in MCT rats were significantly attenuated by treatment with ONO-1301 (Figures 2B and 2C). There were no significant differences in heart rate or mean arterial pressure among the three groups (Table 1).

Representative photomicrographs showed that hypertrophy of the pulmonary vessel wall after MCT injection was attenuated in MCT rats treated with ONO-1301 compared with those given vehicle (Figure 3A). Quantitative analysis demonstrated a significant increase in percent wall thickness after MCT injection, but this change was ameliorated by ONO-1301 (Figure 3B).

Long-Lasting Activity of ONO-1301

We measured plasma ONO-1301 concentrations after a single subcutaneous administration of ONO-1301. The increase in plasma ONO-1301 concentration reached a peak at 4 h, and the half-life of plasma ONO-1301 concentration was approximately 5.6 h (Figure 4). In addition, a single subcutaneous administration of ONO-1301 significantly increased plasma cAMP level in rats (Figure 5). The increase in plasma cAMP level reached a peak at 6 h and lasted at least up to 8 h after ONO-1301 injection. These results suggest that subcutaneous administration of ONO-1301 has long-lasting activity in rats.

Inhibitory Effect of ONO-1301 on Thromboxane Synthase

Although administration of prostacyclin (epoprostenol) markedly increased plasma 11-dehydro-TXB_2 level in MCT rats with established pulmonary hypertension, ONO-1301 did not significantly increase plasma 11-dehydro-TXB_2 level, even after bolus injection (Figure 6A). Plasma 11-dehydro-TXB_2 level was markedly elevated 3 wk after MCT injection (Figure 6B). However, 3-wk treatment with ONO-1301 significantly attenuated the increase in plasma 11-dehydro-TXB_2 level in MCT rats.

Survival Analysis

Kaplan-Meier survival curves demonstrated that MCT rats treated with ONO-1301 had a significantly higher survival rate than MCT rats given vehicle (80 vs. 30% in 6-wk survival; Figure 7).

DISCUSSION

In the present study, we demonstrated that (*1*) a novel prostacyclin agonist (ONO-1301) ameliorated the development of MCT-induced pulmonary hypertension and improved survival in MCT rats; (*2*) ONO-1301 had a long half-life of approximately 5.6 h, and a single administration of ONO-1301 caused a long-lasting increase in plasma cAMP level; and (*3*) ONO-1301 attenuated the increase in plasma 11-dehydro-TXB_2 level in MCT rats.

TABLE 1. PHYSIOLOGIC PROFILES OF EXPERIMENTAL GROUPS

	Sham + Vehicle	MCT + Vehicle	MCT + ONO-1301
No.	10	10	13
BW, g	210 ± 3	159 ± 13*	176 ± 2*
Heart rate, bpm	410 ± 7	400 ± 14	405 ± 16
MAP, mm Hg	122 ± 3	114 ± 5	113 ± 3
RV systolic pressure, mm Hg	36 ± 2	68 ± 4*	47 ± 3*†
RV/BW, g/kg BW	0.58 ± 0.01	0.90 ± 0.05*	0.69 ± 0.03*†
RV/LV + S	0.27 ± 0.01	0.36 ± 0.02*	0.30 ± 0.01†
LV + S/BW, g/kg BW	2.15 ± 0.04	2.52 ± 0.12*	2.26 ± 0.04†

Definition of abbreviations: bpm = beats/minute; BW = body weight; LV + S/BW = ratio of left ventricular plus septal weight to body weight; MAP = mean arterial pressure; MCT = monocrotaline; MCT + ONO-1301, MCT rats treated with ONO-1301; MCT + Vehicle, MCT rats given vehicle; RV = right ventricular; RV/BW = ratio of RV weight to body weight; RV/LV + S = ratio of RV weight to left ventricular plus septal weight; sham + vehicle, sham rats given vehicle.

Data are mean ± SEM.

*$p < 0.05$ versus sham + vehicle.

†$p < 0.05$ versus MCT + vehicle.

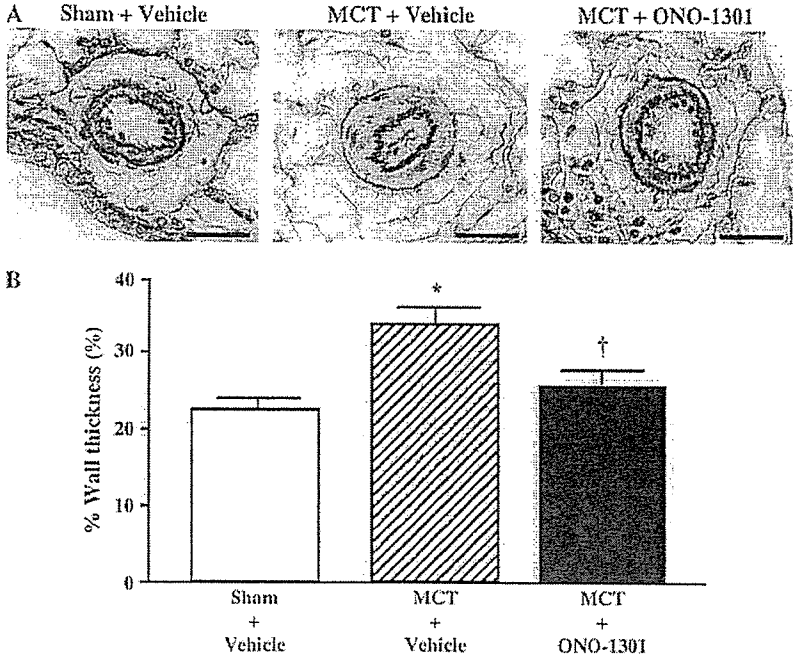

Figure 3. (*A*) Representative photomicrographs of peripheral pulmonary arteries 3 wk after MCT injection. *Scale bars* = 20 μm. (*B*) Quantitative analysis of percent wall thickness in peripheral pulmonary arteries. Data are mean ± SEM. *$p < 0.05$ versus sham + vehicle; †$p < 0.05$ versus MCT + vehicle.

Conventional prostacyclin and its analogs need continuous infusion or frequent administration because of their short duration of acting. Epoprostenol has a very short half-life (< 6 min), iloprost has a serum half-life of 20 to 25 min, and the elimination half-life of beraprost is 35 to 40 min after oral administration (31). Treprostinil sodium, a stable prostacyclin analog, has been reported to have a half-life of 4.6 h after cessation of continuous subcutaneous infusion (32). With regard to cAMP, a second messenger of prostacyclin and its analogs, it has been reported that plasma cAMP levels remained increased at 4 h and normalized at 6 h after inhalation of iloprost (33), and that plasma cAMP levels reached a peak at 30 min and subsequently returned to baseline levels at 2 h after administration of oral beraprost (27). In our results, the half-life of plasma ONO-1301 concentration was approximately 5.6 h, and a single subcutaneous administration of ONO-1301 increased plasma cAMP level at least up to 8 h. Because the method for administration was different between ONO-1301 and conventional prostacyclin analogs (compare a subcutaneous single shot of ONO-1301, continuous intravenous infusion of epoprostenol, continuous subcutaneous infusion of treprostinil, inhalation of iloprost, and oral administration of beraprost), it is difficult to directly compare the lasting effects of prostacyclin activity of ONO-1301 with that of conventional prostacyclin analogs. Nevertheless, the long half-life of ONO-1301 and long-lasting increases in plasma cAMP levels indicate that ONO-1301 exhibits chemical and biologic stability comparable to that of conventional prostacyclin and its analogs. ONO-1301 does not contain prostanoid structures such as a five-membered ring and allylic alcohol, which are subject to metabolism by 15-hydroxyprostaglandin dehydrogenase. These may be the reason for the long-lasting activity of ONO-1301. The present study also demonstrated that repeated administration of ONO-1301 twice per day markedly attenuated the development of MCT-induced pulmonary hypertension, as indicated by significant decreases in RV systolic pressure and RV weight. Thus, intermittent subcutaneous administration of ONO-1301 may be sufficient for the treatment of pulmonary hypertension.

Thromboxane, produced by endothelial cells and platelets, has a potent vasoconstrictor effect, smooth muscle mitogenic property, and platelet aggregation effect (22). Earlier studies

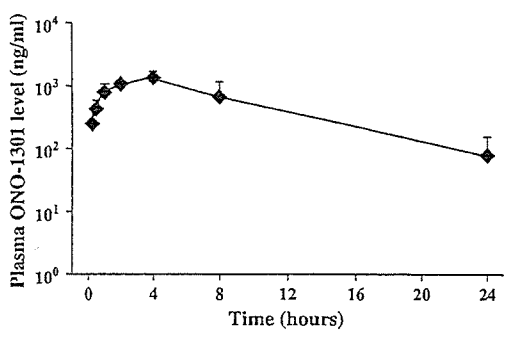

Figure 4. Plasma ONO-1301 concentration after a subcutaneous injection of this compound.

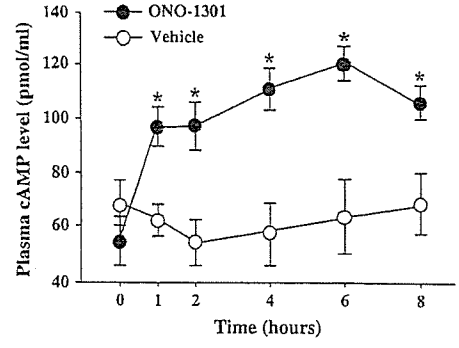

Figure 5. Changes in plasma cAMP level after a single subcutaneous administration of ONO-1301 (*solid circles*) or vehicle (*open circles*). Data are mean ± SEM. *$p < 0.05$ versus vehicle.

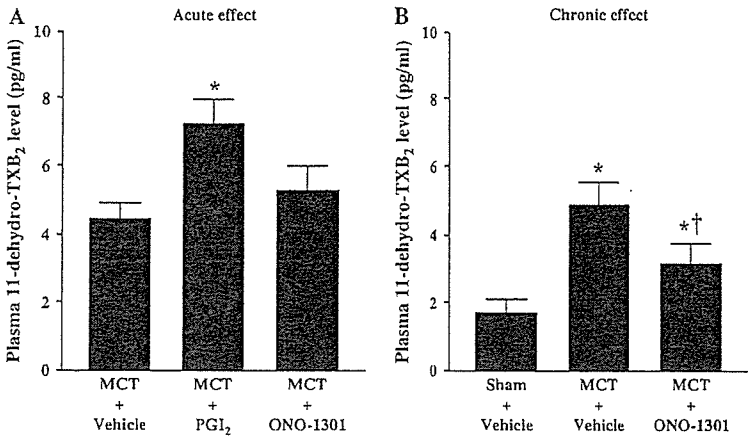

Figure 6. (*A*) Acute effects of ONO-1301 and epoprostenol (PGI_2) on plasma 11-dehydro-thromboxane B_2 (TXB_2), a metabolite of thromboxane A_2, in MCT rats. Data are mean ± SEM. *$p < 0.05$ versus MCT + vehicle. (*B*) Chronic effects of 3-wk treatment with ONO-1301 on plasma 11-dehydro-TXB_2 level. Data are mean ± SEM. *$p < 0.05$ versus sham + vehicle; †$p < 0.05$ versus MCT + vehicle.

have demonstrated impaired prostacyclin synthesis and increased thromboxane production in patients with pulmonary arterial hypertension, suggesting that imbalance of the release of thromboxane and prostacyclin plays an important role in the development of pulmonary hypertension (23, 24). Furthermore, thromboxane-receptor density is increased in the RV of patients with pulmonary hypertension (34). Rich and colleagues have shown that inhibition of thromboxane synthase modestly improves pulmonary hemodynamics in patients with pulmonary arterial hypertension (35). ONO-1301 has a 3-pyridine radical, which is known to inhibit thromboxane synthase through interaction with carboxylic acid via a hydrogen bond. In the present study, plasma 11-dehydro-TXB_2 level was markedly elevated in MCT rats. However, treatment with ONO-1301 greatly diminished its level. Furthermore, in the acute phase, plasma 11-dehydro-TXB_2 level in MCT rats did not significantly increase after administration of ONO-1301, although the plasma level markedly increased after epoprostenol infusion, which is consistent with the earlier study of Cuiper and colleagues (21). Therefore, it is possible that ONO-1301 attenuates MCT-induced pulmonary hypertension partly via improvement of prostacyclin/thromboxane imbalance.

In the present study, ONO-1301 also attenuated the increase in medial wall thickness of peripheral pulmonary arteries. Activation of prostacyclin receptors has been shown to suppress the growth of vascular smooth muscle cells through a cAMP-dependent pathway. Thus, ONO-1301 may attenuate the development of pulmonary vascular remodeling at least in part via a cAMP-dependent pathway. Importantly, repeated administration of ONO-1301 improved survival in MCT rats compared with vehicle administration. The increased survival rate in MCT rats is considered to be associated with the amelioration of pulmonary hypertension. Thus, intermittent subcutaneous administration of ONO-1301 may be an alternative approach for severe pulmonary hypertension refractory to conventional therapy.

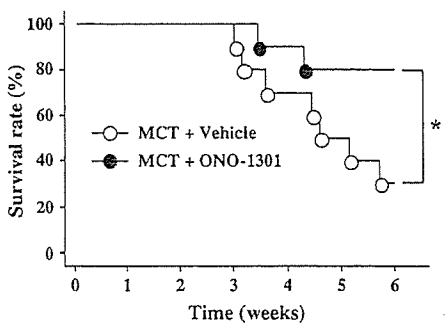

Figure 7. Kaplan-Meier survival curves showing significantly higher survival rate in MCT + ONO-1301 (*solid circles*) than in MCT + vehicle (*open circles*; log-rank test, *$p < 0.05$).

In conclusion, subcutaneous administration of a novel prostacyclin agonist (ONO-1301) markedly attenuated MCT-induced pulmonary hypertension and improved survival in rats. The beneficial effects of ONO-1301 may occur through its long-lasting stimulation of cAMP and inhibition of thromboxane synthase. Thus, administration of this compound may be a promising therapeutic strategy for the treatment of pulmonary arterial hypertension.

Conflict of Interest Statement: None of the authors have a financial relationship with a commercial entity that has an interest in the subject of this manuscript.

References

1. Rich S, Dantzker DR, Ayres SM, Bergofsky EH, Brundage BH, Detre KM, Fishman AP, Goldring RM, Groves BM, Koerner SK, *et al.* Primary pulmonary hypertension: a national prospective study. *Ann Intern Med* 1987;107:216–223.
2. McLaughlin VV, Rich S. Pulmonary hypertension. *Curr Probl Cardiol* 2004;29:575–634.
3. Rich S. Clinical insights into the pathogenesis of primary pulmonary hypertension. *Chest* 1998;114:237S–241S.
4. Archer S, Rich S. Primary pulmonary hypertension: a vascular biology and translational research "work in progress." *Circulation* 2000;102: 2781–2791.
5. Moncada S, Gryglewski R, Bunting S, Vane JR. An enzyme isolated from arteries transforms prostaglandin endoperoxides to an unstable substance that inhibits platelet aggregation. *Nature* 1976;263:663–665.
6. Moncada S, Vane JR. Arachidonic acid metabolites and the interactions between platelets and blood-vessel walls. *N Engl J Med* 1979;300:1142–1147.
7. Nagaya N, Yokoyama C, Kyotani S, Shimonishi M, Morishita R, Uematsu M, Nishikimi T, Nakanishi N, Ogihara T, Yamagishi M, *et al.* Gene transfer of human prostacyclin synthase ameliorates monocrotaline-induced pulmonary hypertension in rats. *Circulation* 2000;102:2005–2012.
8. Rich S, McLaughlin VV. The effects of chronic prostacyclin therapy on cardiac output and symptoms in primary pulmonary hypertension. *J Am Coll Cardiol* 1999;34:1184–1187.
9. Higenbottam T, Wheeldon D, Wells F, Wallwork J. Long-term treatment of primary pulmonary hypertension with continuous intravenous epoprostenol (prostacyclin). *Lancet* 1984;1:1046–1047.
10. Rubin LJ, Mendoza J, Hood M, McGoon M, Barst R, Williams WB, Diehl JH, Crow J, Long W. Treatment of primary pulmonary hypertension with continuous intravenous prostacyclin (epoprostenol): results of a randomized trial. *Ann Intern Med* 1990;112:485–491.

11. Higenbottam TW, Spiegelhalter D, Scott JP, Fuster V, Dinh-Xuan AT, Caine N, Wallwork J. Prostacyclin (epoprostenol) and heart-lung transplantation as treatments for severe pulmonary hypertension. *Br Heart J* 1993;70:366–370.
12. Barst RJ, Rubin LJ, McGoon MD, Caldwell EJ, Long WA, Levy PS. Survival in primary pulmonary hypertension with long-term continuous intravenous prostacyclin. *Ann Intern Med* 1994;121:409–415.
13. Barst RJ, Rubin LJ, Long WA, McGoon MD, Rich S, Badesch DB, Groves BM, Tapson VF, Bourge RC, Brundage BH, *et al.* A comparison of continuous intravenous epoprostenol (prostacyclin) with conventional therapy for primary pulmonary hypertension. *N Engl J Med* 1996;334:296–301.
14. McLaughlin VV, Genthner DE, Panella MM, Rich S. Reduction in pulmonary vascular resistance with long-term epoprostenol (prostacyclin) therapy in primary pulmonary hypertension. *N Engl J Med* 1998;338: 273–277.
15. McLaughlin VV, Shillington A, Rich S. Survival in primary pulmonary hypertension: the impact of epoprostenol therapy. *Circulation* 2002;106: 1477–1482.
16. Sitbon O, Humbert M, Nunes H, Parent F, Garcia G, Herve P, Rainisio M, Simonneau G. Long-term intravenous epoprostenol infusion in primary pulmonary hypertension: prognostic factors and survival. *J Am Coll Cardiol* 2002;40:780–788.
17. Okano Y, Yoshioka T, Shimouchi A, Satoh T, Kunieda T. Orally active prostacyclin analogue in primary pulmonary hypertension. *Lancet* 1997;349:1365.
18. Nagaya N, Uematsu M, Okano Y, Satoh T, Kyotani S, Sakamaki F, Nakanishi N, Miyatake K, Kunieda T. Effect of orally active prostacyclin analogue on survival of outpatients with primary pulmonary hypertension. *J Am Coll Cardiol* 1999;34:1188–1192.
19. Olschewski H, Simonneau G, Galie N, Higenbottam T, Naeije R, Rubin LJ, Nikkho S, Speich R, Hoeper MM, Behr J, *et al.* Inhaled iloprost for severe pulmonary hypertension. *N Engl J Med* 2002;347:322–329.
20. Simonneau G, Barst RJ, Galie N, Naeije R, Rich S, Bourge RC, Keogh A, Oudiz R, Frost A, Blackburn SD, *et al.* Continuous subcutaneous infusion of treprostinil, a prostacyclin analogue, in patients with pulmonary arterial hypertension: a double-blind randomized controlled trial. *Am J Respir Crit Care Med* 2002;165:800–804.
21. Cuiper LL, Patricia VP, Christman BW. Systemic and pulmonary hypertension after abrupt cessation of prostacyclin: role of thromboxane A_2. *J Appl Physiol* 1996;80:191–197.
22. Budhiraja R, Tuder RM, Hassoun PM. Endothelial dysfunction in pulmonary hypertension. *Circulation* 2004;109:159–165.
23. Christman BW, McPherson CD, Newman JH, King GA, Bernard GR, Groves BM, Loyd JE. An imbalance between the excretion of thromboxane and prostacyclin metabolites in pulmonary hypertension. *N Engl J Med* 1992;327:70–75.
24. Adatia I, Barrow SE, Stratton PD, Miall-Allen VM, Ritter JM, Haworth SG. Thromboxane A_2 and prostacyclin biosynthesis in children and adolescents with pulmonary vascular disease. *Circulation* 1993;88: 2117–2122.
25. Itoh T, Nagaya N, Murakami S, Fujii T, Iwase T, Ishibashi-Ueda H, Yutani C, Yamagishi M, Kimura H, Kangawa K. C-type natriuretic peptide ameliorates monocrotaline-induced pulmonary hypertension in rats. *Am J Respir Crit Care Med* 2004;170:1204–1211.
26. Nagaya N, Kangawa K, Kanda M, Uematsu M, Horio T, Fukuyama N, Hino J, Harada-Shiba M, Okumura H, Tabata Y, *et al.* Hybrid cell-gene therapy for pulmonary hypertension based on phagocytosing action of endothelial progenitor cells. *Circulation* 2003;108:889–895.
27. Itoh T, Nagaya N, Fujii T, Iwase T, Nakanishi N, Hamada K, Kangawa K, Kimura H. A combination of oral sildenafil and beraprost ameliorates pulmonary hypertension in rats. *Am J Respir Crit Care Med* 2004;169: 34–38.
28. Sun FF, Taylor BM. Metabolism of prostacyclin in rat. *Biochemistry* 1978;17:4096–4101.
29. Taylor BM, Sun FF. Tissue distribution and biliary excretion of prostacyclin metabolites in the rat. *J Pharmacol Exp Ther* 1980;214:24–30.
30. Catella F, Healy D, Lawson JA, FitzGerald GA. 11-Dehydrothromboxane B_2: a quantitative index of thromboxane A_2 formation in the human circulation. *Proc Natl Acad Sci U S A* 1986;83:5861–5865.
31. Badesch DB, McLaughlin VV, Delcroix M, Vizza CD, Olschewski H, Sitbon O, Barst RJ. Prostanoid therapy for pulmonary arterial hypertension. *J Am Coll Cardiol* 2004;43:56S–61S.
32. Laliberte K, Arneson C, Jeffs R, Hunt T, Wade M. Pharmacokinetics and steady-state bioequivalence of treprostinil sodium (Remodulin) administered by the intravenous and subcutaneous route to normal volunteers. *J Cardiovasc Pharmacol* 2004;44:209–214.
33. Beghetti M, Reber G, de MP, Vadas L, Chiappe A, Spahr-Schopfer I, Rimensberger PC. Aerosolized iloprost induces a mild but sustained inhibition of platelet aggregation. *Eur Respir J* 2002;19:518–524.
34. Katugampola SD, Davenport AP. Thromboxane receptor density is increased in human cardiovascular disease with evidence for inhibition at therapeutic concentrations by the AT(1) receptor antagonist losartan. *Br J Pharmacol* 2001;134:1385–1392.
35. Rich S, Hart K, Kieras K, Brundage BH. Thromboxane synthetase inhibition in primary pulmonary hypertension. *Chest* 1987;91:356–360.

TISSUE ENGINEERING
Volume 11, Number 5/6, 2005

Viability and Osteogenic Potential of Cryopreserved Human Bone Marrow-Derived Mesenchymal Cells

NORIKO KOTOBUKI, M.Sc.,[1] MOTOHIRO HIROSE, Ph.D.,[1] HIROKO MACHIDA, M.Sc.,[1] YOUICHI KATOU, B.Sc.,[1] KAORI MURAKI, B.Sc.,[1] YOSHINORI TAKAKURA, M.D.,[2] and HAJIME OHGUSHI, M.D.[1]

ABSTRACT

Human bone marrow-derived mesenchymal cells contain mesenchymal stem cells (MSCs), which are well known for their osteo/chondrogenic potential and can be used for bone reconstruction. This article reports the viability of cryopreserved human mesenchymal cells and a comparison of the osteogenic potential between noncryopreserved and cryopreserved human mesenchymal cells with MSC-like characteristics, derived from the bone marrow of 28 subjects. The viability of cryopreserved mesenchymal cells was approximately 90% regardless of the storage term (0.3 to 37 months). It is clear by fluorescence-activated cell sorter analysis that the cell surface antigens of both noncryopreserved and cryopreserved mesenchymal cells were negative for hematopoietic cell markers such as CD14, CD34, CD45, and HLA-DR but positive for mesenchymal characteristics such as CD29 and CD105. To monitor the osteogenic potential of the cells, such as alkaline phosphatase (ALP) activity and *in vitro* mineralization, a subculture was conducted in the presence of dexamethasone, ascorbic acid, and glycerophosphate. No difference in osteogenic potential was found between cells with or without cryopreservation treatment. In addition, cells undergoing long-term cryopreservation (about 3 years) maintained high osteogenic potential. In conclusion, cryopreserved as well as noncryopreserved human mesenchymal cells could be applied for bone regeneration in orthopedics.

INTRODUCTION

MESENCHYMAL STEM CELLS (MSCs) are multipotent cells and can be induced *in vitro* and *in vivo* to differentiate into various functional cell types of mesodermal tissues including bone, cartilage, tendon, fat, and bone marrow stroma.[1–3] Many researchers, including us, have previously reported that primary cultures of mesenchymal cells derived from bone marrow could differentiate into osteoblasts by treatment with dexamethasone (Dex). The osteoblasts formed extracellular bone matrices with abundant minerals on ceramic surfaces.[4–6] On the basis of these results, it has been proposed that autologous mesenchymal cells be used for the treatment of bone/joint diseases.[7] The mesenchymal cells can differentiate into osteoblasts not only on tissue culture polystyrene (TCPS) dishes but also on the surfaces of biomaterials, such as bioactive calcium phosphate ceramics and bioinert alumina ceramics.[8] "Regenerative cultured bone tissue," which is a hybrid of culture-differentiated osteoblasts/bone matrix on biomaterials, has already been implanted into patients.[9]

[1]Research Institute for Cell Engineering (RICE), National Institute of Advanced Industrial Science and Technology (AIST), Amagasaki, Hyogo, Japan.
[2]Department of Orthopedic Surgery, Nara Medical University, Kashihara, Nara, Japan.

Studies have also demonstrated the possibility that MSCs can differentiate into other types of tissue-specific cells such as cardiac myoblasts,[10] vascular endothelial cells,[11,12] hepatocytes,[13] and neural cells.[14] These results indicate the usefulness of multipotential MSCs for tissue-engineering purposes in regenerative medicine.[15,16] Bone marrow cells have been utilized as a source of MSCs; however, the number of MSCs to be culture-expanded from fresh bone marrow in a short time is limited and the MSCs cannot survive for long periods under culture conditions. Because MSCs are difficult to isolate from bone marrow, because of the paucity of specific markers, we have used whole adherent cells (mesenchymal cells) from bone marrows that showed high osteogenic potential.

As the technology to preserve cultured cells by freezing methods has progressed,[17,18] cryopreserved cells have been expected to become cell sources for the fabrication of regenerative tissues and to have potentially important implications for clinical applications in regenerative medicine. This is especially significant because of the limited supply of mesenchymal cells. Therefore, if long-term cryopreserved mesenchymal cells still retain a high level of viability and ability to differentiate into tissue-specific cells, they will be useful as a cell source to regenerative medicine, especially autologous usage to avoid transplantation immunity, not only for bone but also other tissue reconstruction therapy.

We have previously reported that cryopreserved human mesenchymal cells after thawing had more than 90% viability and differentiated into osteoblasts in the presence of Dex.[19] However, only three cases were analyzed and we did not analyze the entire number of cryopreserved cells, only the adherent cells. In this study, we report direct evidence of the viability and osteogenic potential of cryopreserved mesenchymal cells, from 28 donors, which were stored for 0.3 to 37 months. We also compared cell morphology, expression of cell surface antigens, and osteogenic activities between cryopreserved and noncryopreserved mesenchymal cells derived from fresh bone marrow of the same donors.

MATERIALS AND METHODS

Cell preparation and culture method

In accordance with the Ethics Committee at the Tissue Engineering Research Center (Amagasaki, Japan), we obtained informed consent from the bone marrow donors. The age, gender, and results of biological assays of each donor are listed in Table 1. Three milliliters of bone marrow was captured in a 13-mL tube (Assist, Tokyo, Japan) containing the same volume of heparinized (10 U/mL) phosphate-buffered saline (PBS; Invitrogen, Carlsbad, CA). The mixture of bone marrow and heparinized PBS was centrifuged at 140 × *g* for 10 min at 4°C and the supernatant of plasma with the fat layer was discarded. The residue (buffy coat together with the red blood cell layer) was put into 75-cm^2 flasks (BD Biosciences Discovery Labware, Bedford, MA) with basal medium comprising Eagle's minimal essential medium α (α-MEM; Invitrogen) containing 15% fetal bovine serum (FBS; JRH Biosciences, Leneka, KS) and antibiotics, and then cultured in a humidified atmosphere of 95% air with 5% CO_2 at 37°C.[20]

At subconfluency, the cell density is about 2.5–6.5 × 10^4 cells/cm^2; the mesenchymal cells are detached from the flasks with 0.05% trypsin–0.53 mM EDTA (Invitrogen), concentrated at a density of 5 × 10^5 cells/mL, and suspended in Cell Banker storage solution (Juji Field, Tokyo, Japan), a ready-to-use storage solution containing dimethyl sulfoxide (DMSO) and fetal bovine serum. As a simplified process of program freezing, mesenchymal cells in the storage solution were stored sequentially at 4°C for 10 min, −30°C for 1 h, and −80°C for 2–3 days. Finally, mesenchymal cells were stored at −152°C for long-term cryopreservation. Noncryopreserved mesenchymal cells from 15 samples (Table 1, nos. 12, 13, and 16–28) and cryopreserved mesenchymal cells from 26 samples (Table 1, nos. 1–6 and 9–28) were seeded on a 12-well plate at a cell density of 1 × 10^4/cm^2 and cultured under osteogenic conditions for 2 weeks. The culture medium was changed three times per week. The osteogenic medium contained 10 mM β-glycerophosphate disodium salt (β-GP; Merck, Darmstadt, Germany), 0.07 mM L-ascorbic acid 2-phosphate magnesium salt n-hydrate (Sigma-Aldrich, St. Louis, MO), and 0.1 μM Dex (Sigma-Aldrich) in the basal medium. In addition, calcein (1 μg/mL; Dojindo Laboratories, Kumamoto, Japan) was included in the medium for one of the osteogenic assays, quantitative analysis of calcium contents. As a negative control, cells were cultured in basal medium containing only 10 mM β-GP.

FACS analysis

Cells noncryopreserved before subculture and cells cryopreserved immediately after thawing were incubated with each fluorescein isothiocyanate (FITC)-conjugated anti-cluster of differentiation (CD) antibody on ice for 30 min in the dark. After the wash step, the cells were loaded in a FACSCalibur flow cytometer (BD Biosciences Immunocytometry Systems, San Jose, CA) with a minimum of 10,000 events counted. The antibodies used in this experiment were to CD14, CD34, CD45 (Caltag Laboratories, Burlington, CA), CD29, CD105, and human leukocyte antigen region DR (HLA-DR) (Serotec, Oxford, UK). Mouse immunoglobulin G (IgG) (Beckman Coulter, Fullerton, CA) was used as an isotype control. The fluorescence intensity of each antibody was compared

TABLE 1. DONOR INFORMATION AND VIABILITY AND OSTEOGENIC ACTIVITIES OF NONCRYOPRESERVED AND CRYOPRESERVED HUMAN MESENCHYMAL CELLS[a]

			Noncryopreserved cells				*Cryopreserved cells*					
			ALP/DNA (μmol/μg)		*Calcein (FI/area)*		*Cell viability*	*Storage period*	*ALP/DNA (μmol/μg)*		*Calcein (FI/area)*	
ID	*Age (years)*	*Sex (F/M)*	*Dex (+)*	*Dex (−)*	*Dex (+)*	*Dex (−)*	*(%)*	*(months)*	*Dex (+)*	*Dex (−)*	*Dex (+)*	*Dex (−)*
1	71	M					81.2	33.3	2.72	0.37	2,909	286
2	27	M					92.8	33.3	0.65	0.11	595	128
3	65	F					87.8	33.6	0.6	0.17	3,057	216
4	66	F					82.9	33	0.66	0.34	3,618	306
5	55	F					89.3	37.3	0.55	0.21	1,613	173
6	77	F					89.3	37	0.53	0.17	5,319	287
7	62	F					99	36				
8	55	F					100	23.6				
9	66	F					83	15	0.166	0.086	3,288	1,747
10	70	F					94.6	15	0.194	0.044	1,980	426
11	61	M					100	12	0.222	0.023	157	112
12	62	M	0.185	0.086	4,190	214		6	0.16	0.05	5,436	132
13	54	F	0.358	0.106	5,900	2,620		7	0.13	0.1	3,117	147
14	71	M						0.6	0.03	0.01	1,971	125
15	70	F					91.1	6	0.851	0.064	4,027	2,131
16	69	F	0.119	0.091	9,017	99		0.3	0.09	0.02	812	120
17	58	M	0.172	0.081	11,994	88		1.3	0.2	0.08	6,526	156
18	25	M	0.307	0.042	6,740	53		1.3	0.34	0.06	3,591	171
19	75	F	0.278	0.086	10,168	42		1.3	0.36	0.14	3,263	201
20	42	M	0.471	0.124	3,027	68	71.9	5.3	0.322	0.061	5,267	131
21	42	M	0.573	0.001	4,746	4,836	84.9	5.5	0.24	0.178	2,741	889
22	72	F	0.27	0.085	3,156	33	92.2	5.6	0.289	0.125	2,149	355
23	14	M	0.322	0.072	2,447	26	91.4	5	0.453	0.047	1,243	33
24	77	M	0.21	0.124	3,317	114	96.4	4.3	0.472	0.405	2,501	189
25	8	M	0.417	0.312	4,918	1,140	88	5	0.63	0.058	2,800	97
26	83	M	0.405	0.14	5,528	216	98.3	4.3	0.55	0.064	4,208	107
27	70	F	0.33	0.077	9,719	231	95.6	3.6	0.912	0.216	2,206	143
28	29	M	0.687	0.113	5,020	301	85.4	3	0.815	0.078	4,096	134

[a]Independent donors are listed by ID numbers. Mesenchymal cells were cultured with or without Dex for 2 weeks. ALP activity was measured by enzymatic reaction using pNPP. Calcium deposition was measured by detecting the fluorescence intensity (FI) of calcein deposited in the extracellular matrix of the cell culture. All data represent the mean of six independent experiments. The viability of stored (cryopreserved) cells immediately after thawing was measured with a NucleoCounter. Blanks, no data.

with that of the isotype control and represented as a histogram.

Cell viability assay

The viability of cryopreserved cells from 21 samples (Table 1, nos. 1–11, 15, and 20–28) was analyzed with a NucleoCounter (ChemoMetec, Allerød, Denmark). Because the detection principle is based on staining nuclei with a dye, it is evident that in order to stain the nuclei they must be permeable to the dye. The dye cannot penetrate a viable cell and thus it is necessary to lyse the cell membrane before staining. Nonviable cells, on the other hand, are permeable and can therefore be stained with the nuclear dye. Using this property of nonviable cells and combining results obtained from samples that have not been lysed (nonviable cell count) and the result obtain by lysing cells (a total cell count), it becomes possible to use the NucleoCounter to estimate the viability of a cell sample.

Immediately after thawing, cryopreserved cells were diluted by a factor of 10 with culture medium. Cell suspensions were centrifuged at 400 × *g* for 5 min and resuspended with 5 mL of culture medium. Two hundred microliters of each cell sample was analyzed on the NucleoCounter with cartridges before and after treatment with a lysis buffer, giving an estimate of nonviable and total cells, respectively. The manual counting method was based on the trypan blue exclusion procedure.

Alkaline phosphatase activity assay

The alkaline phosphatase (ALP) activity of cultured cells from 15 samples of noncryopreserved cells (Table 1, nos. 12, 13, and 16–28) and 26 samples of cryopreserved cells (Table 1, nos. 1–6, and 9–28) was examined by the specific conversion of *p*-nitrophenyl phosphate (pNPP) into *p*-nitrophenol (pNP). Reddi and Sullivan have described the method in detail[21]; minor modifications to the method have been described in our previous reports.[22] Briefly, cells scraped into 0.5 mL of ice-cold 10 mM Tris-HCl, 1 mM EDTA, and 100 mM NaCl (pH 7.4) were sonicated and used for measurement of DNA. The DNA contents of the cells were measured with Hoechst 33258 (molecular probe). Twenty microliters of suspended cell solution was added to 0.2 mL of buffer containing Hoechst 33258 (5 μg/mL) and the fluorescence was measured on a microplate reader (Wallac 1420 ARVOsx; PerkinElmer Life and Analytical Sciences, Boston, MA). Standard DNA solutions were prepared with salmon sperm DNA (Invitrogen). After measured DNA contents, sonicated cell solution was centrifuged at 10,000 $\times$ *g* for 1 min at 4°C. An aliquot (20 μL) of the supernatant was assayed for ALP activity, using pNPP solution (Zymed Laboratories, South San Francisco, CA). The cell solutions were incubated at 37°C for 30 min and measured on the microplate reader for absorbance of the pNP product formed at 405 nm. Enzyme activity was expressed as micromoles of pNP produced per 30 min per DNA content. Data represent the mean of at least six independent trials.

Image analysis and calcium assay of extracellular mineralization

Extracellular mineralization by the cells was visualized with calcein, which is a calcium-binding fluorescent chemical used to detect bone minerals. The fluorescence intensity of calcein showed excellent correlations with calcium content.[23,24] Calcein (1 μg/mL) was added to the medium for entire culture periods. The medium containing calcein was removed and cells were washed with PBS immediately before these analyses. The fluorescence of calcein incorporated into extracellular mineral ingredients was visualized and quantified with an image analyzer (Typhoon 8600; 526 nm short-pass filter; Amersham Biosciences, Piscataway, NJ). The scanned fluorescent images were quantitated with ImageQuant TL software (Amersham Biosciences) and represented as intensity per area. We calculated the area under the curve created by a plot of the pixel intensities and the pixel locations along a linear object, such as a line. ImageQuant displays the pixel intensities as a line graph. The results were transferred to Excel (Microsoft, Redmond, WA) and calculated the pixel intensities per selected area. Extracellular mineralization was also observed with a fluorescence microscope (Olympus IX70; Olympus Optical, Tokyo, Japan) as well as a phase-contrast microscope. Data represent the mean of at least six independent experiments.

Statistical data analysis

For statistical analysis of the flow cytometry data, a Kolmogorov–Smirnov (KS) two-sample test was used for the two histograms resulting from gating the following populations[25]: KS statistics calculated by the CellQuest software program (BD Biosciences Immunocytometry Systems) on the whole histograms produced the index of similarity *D*/*s*(*n*) and a *D* value (Table 2). As for ALP activity per DNA contents and calcium deposition, a two-tailed Student *t* test computed by JMP 5.0 software (SAS Institute, Cary, NC) was used to determine the statistical significance of the measured differences. Error bars shown in Figs. 3 and 5 indicate the standard deviation (SD). The relationship between cell viability and storage period was displayed in a scatter diagram and the regression line and equation were included in the diagram (Fig. 4).

RESULTS

Human bone marrow cells from 28 patients were cultured to expand mesenchymal cells. The 15 samples of subcultured mesenchymal cells without cryopreservation were maintained for 14 days in osteogenic medium. The degrees of viability of 21 cases of cryopreserved mesenchymal cells were checked immediately after thawing and then subcultured in the same way. Information related to the 28 donors is listed in Table 1.

For analyses of cell surface antigens, both cryopreserved and noncryopreserved cells were negative for hematopoietic stem cell markers CD34, CD45, hematopoietic cell marker CD14, and HLA-DR. However, the cells were strongly positive for CD29 and CD105, all of which are commonly used in the analyses of MSCs. These data coincide well with the reported data of MSC characteristics.[26–32] The analysis also revealed no distinct differences between noncryopreserved and cryopreserved mesenchymal cells (Fig. 1). Furthermore, Kolmogorov–Smirnov (KS) statistics were applied to overlaid histograms between isotype control and each cell surface antibody. This resulted in an index of each pair of curves (Fig. 1), indicating the similarity between noncryopreserved cells and cryopreserved cells ($p < 0.001$) in all cases (Table 2).

To check whether cryopreserved mesenchymal cells have proliferation/osteogenic differentiation capabilities comparable to those of noncryopreserved mesenchymal cells, a 14-day subculture was conducted in the presence or absence of Dex. The expression of ALP changed in a

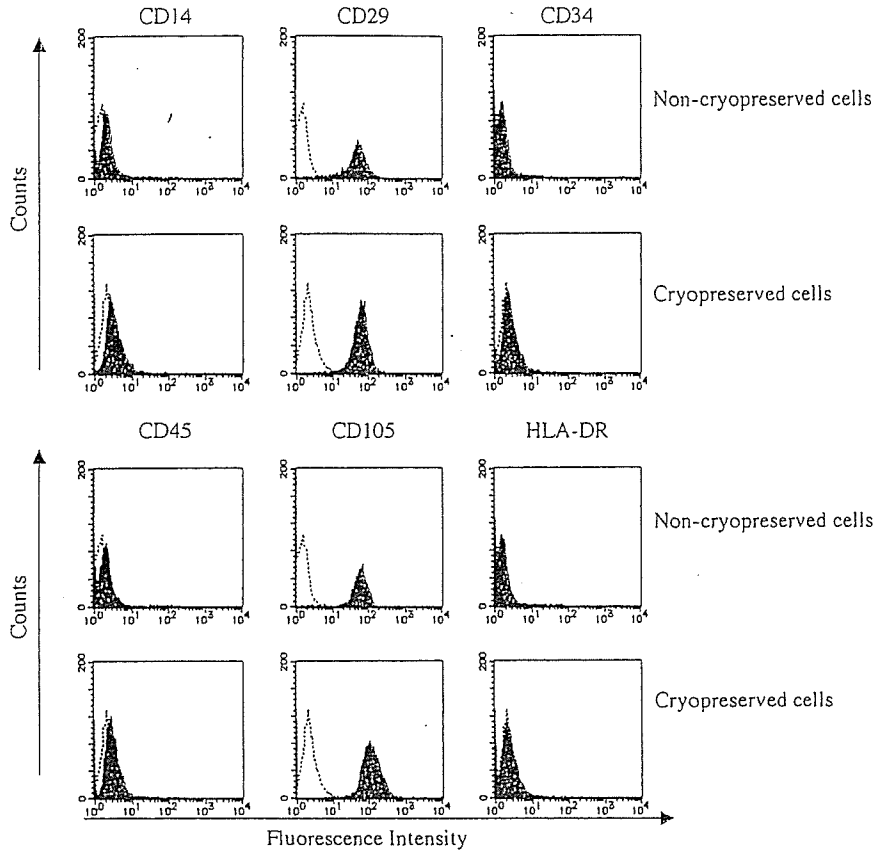

FIG. 1. FACS analyses of noncryopreserved and cryopreserved human mesenchymal cells. Noncryopreserved cells derived from no. 28 and cryopreserved cells derived from no. 9 are represented here. These cells were labeled with FITC-conjugated antibodies against CD14, CD29, CD34, CD45, CD105, HLA-DR, or immunoglobulin G isotype control antibodies. Cells were analyzed with a FACSCalibur. The *x* axis indicates fluorescence intensity (FI). The *y* axis indicates cell counts. Open and solid histograms indicate the results using isotype control immunoglobulin G and specific antibodies, respectively.

TABLE 2. KOLMOGOROV–SMIRNOV TWO-SAMPLE TEST[a]

		KS Two-sample test	
CD marker	*Variable*	*Noncryopreserved cells*	*Cryopreserved cells*
CD14	*D/s(n)*	25.56	26.67
	D	0.42	0.38
CD29	*D/s(n)*	52.82	70.25
	D	0.99	1
CD34	*D/s(n)*	6.71	11.03
	D	0.11	0.16
CD45	*D/s(n)*	19.87	21.45
	D	0.33	0.3
CD105	*D/s(n)*	52.89	69.87
	D	0.99	1
HLA-DR	*D/s(n)*	3.62	3.48
	D	0.06	0.05

[a]The calculation computes the summation of the curves and finds the greatest difference between the summation curves (p 0.001). All indexes of the Kolmogorov–Smirnov two-sample test show the difference between the histogram of CD markers and that of isotype control (see Fig. 1). *D/s(n)*, index of similarity for two curves; *D*, KS statistic (simply, the greatest difference between the two curves). If the indexes of both noncryopreserved cells and cryopreserved cells are close to each other, this means both histograms shown in Fig. 1 are similar to each other.

time-dependent manner and reached a plateau on days 7–11 cultivation. Furthermore, calcium deposition started from day 11 to 14 of cultivation (data not shown). Those time lags were caused by the difference in cell origin, in other words, the condition of the patient. We consequently fixed on day 14 for the analysis because both ALP activity and calcium deposition could be analyzed at one time, even if the plateau in ALP activity was missed by a little.

Calcein enabled us to analyze calcium deposition quantitatively, using an image analyzer (Fig. 2A amd B, panels a), as well as to visualize calcium deposition by fluorescence microscopy (Fig. 2A and B, panels b). The fluorescence intensity of calcein showed excellent correlation with calcium contents as described in Materials and Methods. Furthermore, calcein is easily used in a quantifiable approach to calcium deposition.[23,24] We therefore performed only the calcein assay for calcium deposition. As shown in panels a of Fig. 2, culturing with Dex showed abundant mineralization (calcein uptake) over the entire area of the TCPS as detected with the image analyzer. Mineralization was similarly observed in both noncryopreserved cells (Fig. 2A) and cryopreserved cells (Fig. 2B). Detailed morphology is shown in Fig. 2 by fluorescence and phase-contrast microscopy (panels b and c, respectively). Amorphous mineralized nodular aggregates, seen in panels c of Fig. 2 [Dex(+)], coincided with the fluorescent areas [panels b of Fig. 2, Dex(+)], indicating areas of calcein uptake. When these cells were cultured in the absence of Dex, mineralization was not detected [Fig. 2, Dex(–)]. These patterns of extracellular mineralization were similarly seen in both noncryopreserved and cryopreserved cells.

As shown in Fig. 3, ALP activity and calcein uptake of noncryopreserved mesenchymal cells from 15 cases

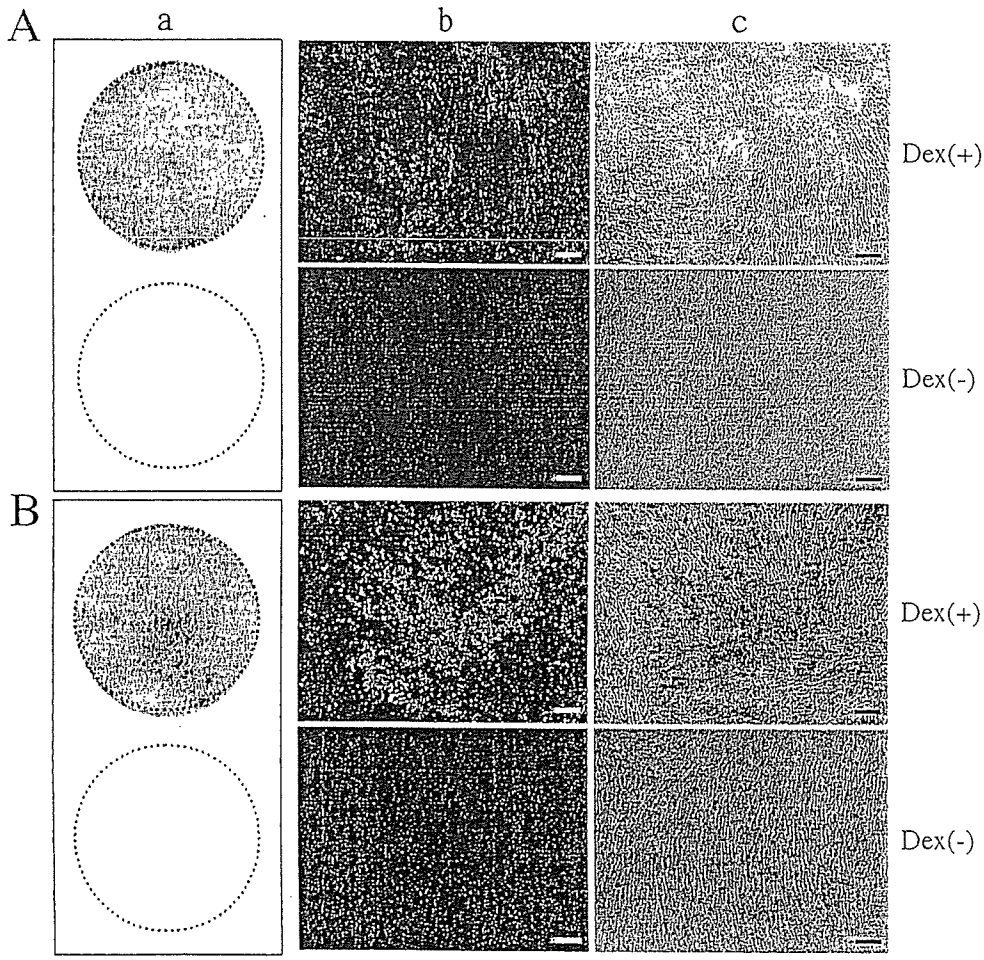

FIG. 2. Cell morphology and mineralization capacity of noncryopreserved and cryopreserved human mesenchymal cells. The noncryopreserved (A) and cryopreserved (B) cells represented here were derived from sample no. 27. The cells were cultured for 2 weeks in the presence of calcein with (+) or without (−) Dex. Calcium deposition (a) detected by calcein uptake was visualized with an image analyzer. The round area indicates the entire area of the well in 12-well plates. Each micrograph represents a fluorescence image (b) or a phase-contrast image (c). Original magnification: (b and c) ×100. Scale bars: 200 μm.

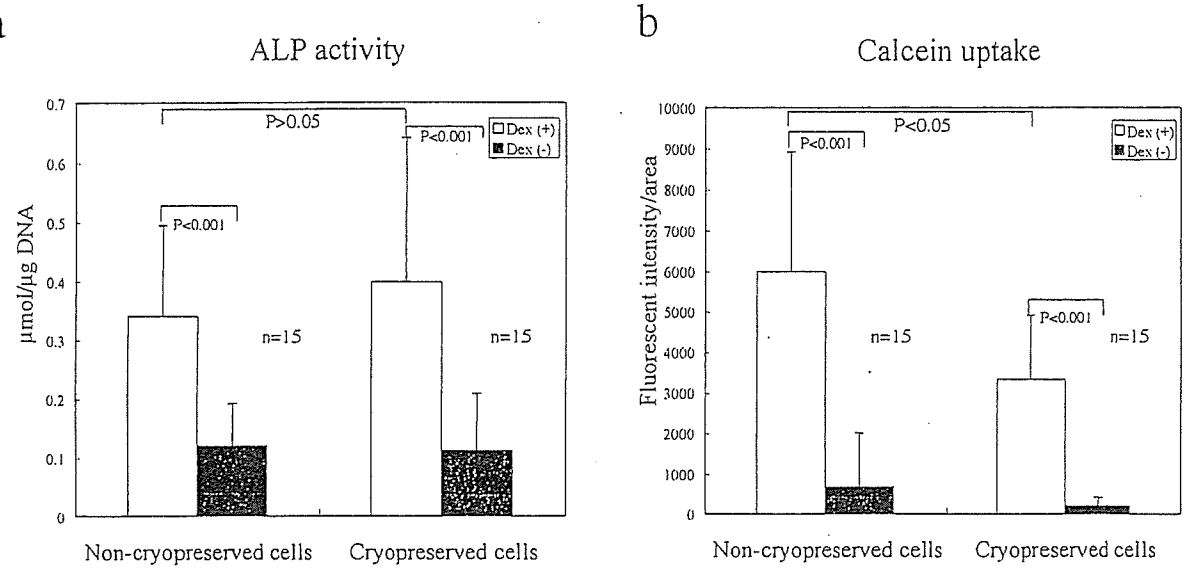

FIG. 3. Osteogenic activities of noncryopreserved and cryopreserved human mesenchymal cells. Fifteen samples of noncryopreserved cells and 15 corresponding samples of cryopreserved cells (nos. 12, 13, and 16–28) are represented with standard deviations (SD). (a) ALP activity (μmol/μg DNA) ($p = 0.448$); (b) calcein uptake (fluorescence intensity) ($p = 0.004$). Open columns indicate the data of cells cultured in the presence of Dex; solid columns indicate the data of cells cultured in the absence of Dex. Data for the two groups, that is, culturing in the presence or absence of Dex, were examined at a level of significance of $p < 0.001$.

and the biochemical parameters of cryopreserved mesenchymal cells from 15 corresponding cases were measured quantitatively. As for both ALP activity and calcium deposition, both types of mesenchymal cells showed Dex-dependent differentiation. A significant difference between noncryopreserved and cryopreserved cells was not seen in the case of ALP activity ($p > 0.05$). This result indicates that cryopreservation has no influence on the ability of mesenchymal cells to undergo osteoblastic differentiation. However, calcium uptake showed some difference between noncryopreserved and cryopreserved cells ($p < 0.05$).

We analyzed the cell viability of 21 samples (cryopreserved from 0.3 to 37 months) immediately after thawing (Fig. 4). The average cell viability was about 90% (range, 71.9–100%). Application of a straight line to this scatter resulted in $y = -0.0081x + 90.405$, and $R^2 = 0.0002$. These results show that mesenchymal cells can maintain viability in spite of long-term storage.

As shown in Fig. 5, we compared the osteogenic activities (ALP activity and calcein uptake) of 16 samples stored for less than 6 months (defined as short-term) with those of 6 samples stored for 33 to 37 months (defined as long-term). Both groups of mesenchymal cells differentiated Dex dependently, but no significant difference between noncryopreserved and cryopreserved cells was seen ($p > 0.05$). These results show that not only short-term but also long-term cryopreserved mesenchymal cells could maintain their capabilities for osteogenic differentiation.

DISCUSSION

With the rapid advancements in tissue engineering, a multitude of applications for cultured cells in construction of regenerative cultured tissues has been discovered.[3,33] Cultured cells have been used for cell-based therapy and fabrication of tissue-engineered devices. In this regard, we have already been involved in more than 30 cases of human mesenchymal cells from donors to fabricate *in vitro*-cultured regenerative bone for the treatment of various skeletal diseases including arthritis, bone tumors, and osteonecrosis. The cultured mesenchymal cells used for cell-based therapy were all autologous cultured cells without cryopreservation. Some cases, such as arthritis of both the left and right sides, required duplicate treatments with mesenchymal cells and some cases required multiple harvests of fresh bone marrow to expand the number of mesenchymal cells. Therefore, cryopreserved mesenchymal cells that retain a high degree of viability and osteogenic activities, equal to that of primary cultured mesenchymal cells, could be used for such subjects, thus avoiding the risk and possible damage caused by multiple marrow harvests. Furthermore, early bone marrow collection may be highly effective because it is also described that young bone marrow contains more mesenchymal cells than that harvested from older patients.[34] Thus, mesenchymal cells harvested from young patients could be cryopreserved like a "cell bank" with high proliferation and differentiation capabilities and

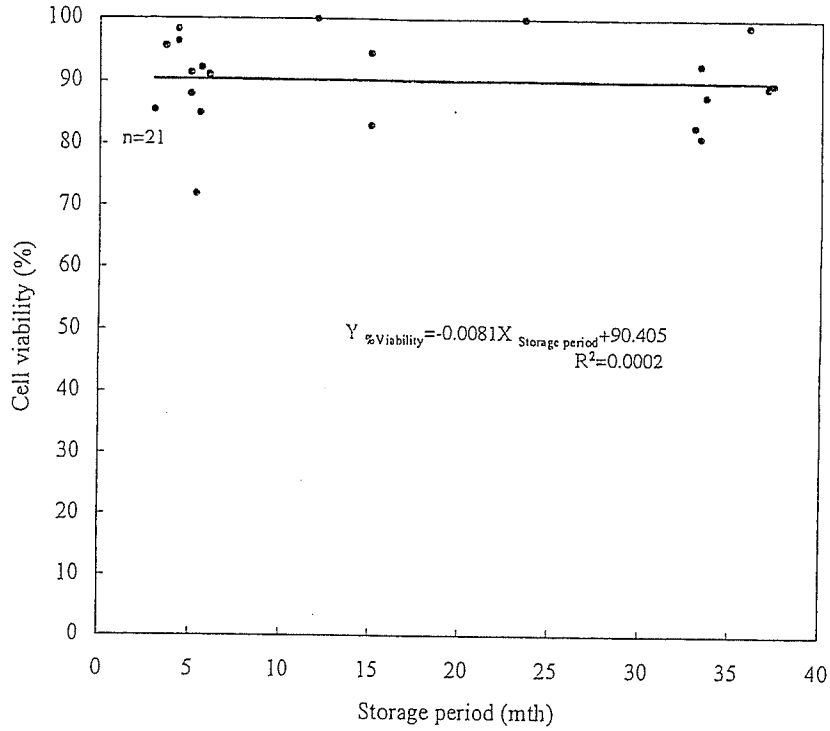

FIG. 4. Viability of cryopreserved human mesenchymal cells relative to storage period. Twenty-one samples of cryopreserved human mesenchymal cells derived from samples 1–11, 15, and 20–28 (see Table 1) were used for determination of cell viability. Immediately after thawing of the cells, cell viability was evaluated with a NucleoCounter. The approximate curve is $y = -0.0081x + 90.405$. $R^2 = 0.0002$. The correlation coefficient is −0.0141.

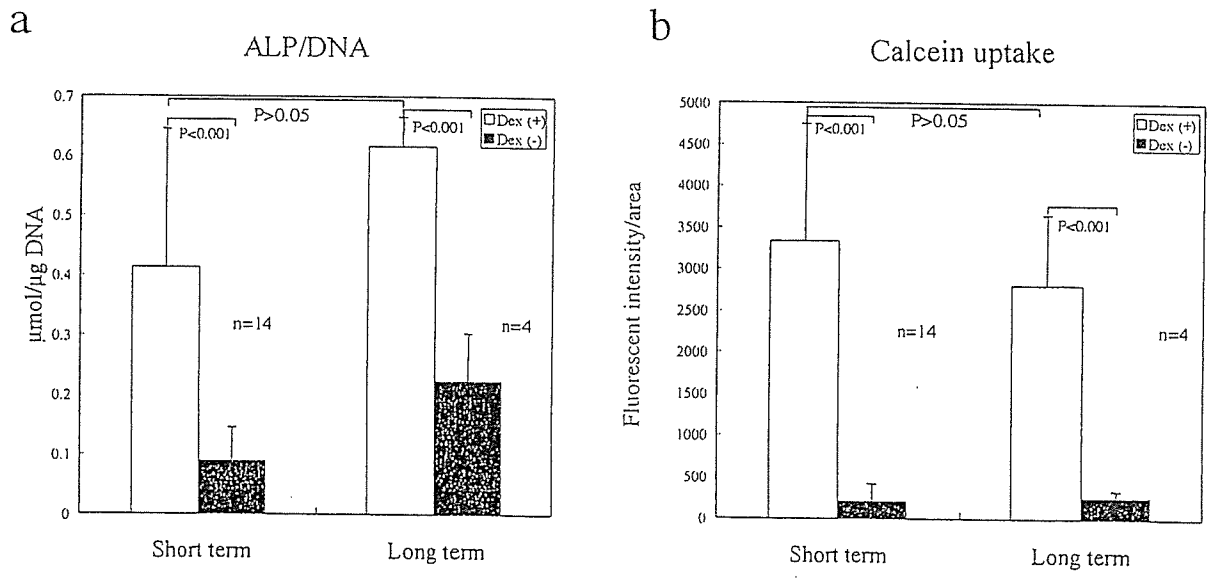

FIG. 5. Osteogenic potential of short-term and long-term cryopreserved human mesenchymal cells. Sixteen samples of short-term cryopreserved cells (nos. 12 and 14–28) and 6 samples (nos. 1–6) of long-term cryopreserved cells are represented. (a) ALP activity (μmol/μg DNA) ($p = 0.129$); (b) calcein uptake (fluorescence intensity) ($p = 0.185$). Open columns indicate the data of cells cultured in the presence of Dex; solid columns indicate the data of cells cultured in the absence of Dex. The highest and lowest values were not counted by rejection test and the error bars show the standard deviation (SD). Data of the two groups, that is, cultured in the presence or absence of Dex, were examined at a level of significance of $p < 0.001$.

used for future treatment of the same individual. Therefore, if cryopreserved mesenchymal cells were managed at a cell bank, it would be easy to supply numerous MSCs should such be needed.

In this report, we demonstrated the viability of cryopreserved mesenchymal cells. After storage for more than 3 years, cryopreserved cells had a surprisingly high degree of viability, (about 90%), indicating that long-term cryopreservation for several months is not a critical problem. This durability may reflect the nature of the stem cells used in our MSC preparation. Most of these living cells attached to culture-grade dishes in a manner similar to primary cultured cells. The attached cells proliferated well and showed a high degree of osteogenic activity, comparable to that of primary cultured cells. We believed that the calcium deposition level of cryopreserved cells would be similar to that of noncryopreserved cells because cryopreserved cells show the same level of ALP activity compared with noncryopreserved cells (Fig. 3). The amount of calcium deposition derived from cryopreserved cells may be supplemented by additional cultivation. Although the data indicated individual differences in cell viability and osteogenic activities, long-term cryopreservation did not seriously affect these aspects. The results clearly showed that cryopreserved mesenchymal cells could be stored and maintain high degrees of viability and osteogenic potential. Furthermore, the cryopreserved cells were morphologically, phenotypically, and functionally comparable to primary cultured mesenchymal cells. In conclusion, we believe that cryopreserved mesenchymal cells could become a promising candidate cell source for the fabrication of regenerative bone tissues available for a wide range of solutions to bone/joint problems.

Cryopreservation of tissue and cells is a technique that has been utilized by scientists since the 1700s. This process puts the cells in suspended animation, a state in which they can retain their viability indefinitely. In the mid-1900s, the science of cryobiology improved rapidly with the discovery of the beneficial effects of cryoprotectant substances added to cell-freezing solutions. Cryopreservation is now routinely used to store semen, embryos, and all types of cells/tissues from animals and humans. Before freezing, the cells must be treated with a cryoprotectant solution (DMSO or glycerol). These substances protect the cells and their membranes from damage during the freezing process. On the other hand, it has been reported that DMSO is not only cytotoxic but also induces neuron-like cells[35] or cardiac myocytes[36] when added to culture medium. Some groups use a nontoxic cryoprotectant solution such as trehalose in place of DMSO for the cryopreservation of stem cell.[37] In this study, we used DMSO as a cryoprotectant solution and we confirmed that thawed mesenchymal cells had, on average, 90% viability and did not show DMSO-dependent differentiation after cryopreservation (data not shown). But it is surely important to take other cryoprotectant solutions into consideration, because mesenchymal cell must be kept safely for clinical use.

Although it is still difficult to control the differentiation of MSCs with any humoral factors, it has currently been reported that MSCs have multipotentiality as evidenced by their ability to differentiate into numerous cell types such as cardiac myoblasts,[10] vascular endothelial cells,[11,12] hepatocytes,[13] and neural cells.[14] Our current, ongoing study has demonstrated cardiac/vascular regeneration and hepatocyte differentiation using cryopreserved human mesenchymal cells. This study together with other data, clearly demonstrate the excellent viability and differentiative ability of cryopreserved human mesenchymal cells. Consequently, cryopreserved mesenchymal cells may also be applied in the field of regenerative medicine for liver, heart, and vascular regeneration as an MSC source.

ACKNOWLEDGMENTS

This work was supported by the Three-Dimensional Tissue Module Project of METI (a Millennium Project) and a Grant-in-Aid for Scientific Research. We thank Dr. Mitsuo Oshimura (Division of Molecular Genetics and Biofunction, Tottori University) for valuable discussion.

REFERENCES

1. Maniatopoulos, C., Sodek, J., and Melcher, A.H. Bone formation *in vitro* by stromal cells obtained from bone marrow of young adult rat. Cell Tissue Res. 254, 317, 1988.
2. Le Douarin, N.M., Houssaint, E., Jotereau, F.V., and Belo, M. Origin of hemopoietic stem cells in embryonic bursa of Fabricius and bone marrow studied through interspecific chimeras. Proc. Natl. Acad. Sci. U.S.A. 72, 2701, 1975.
3. Caplan, A.I., and Bruder, S.P. Mesenchymal stem cells: Building blocks for molecular medicine in the 21st century. Trends Mol. Med. 7, 259, 2001.
4. Ohgushi, H., Okumura, M., Tamai, S., Shors, E.C., and Caplan, A.I. Marrow cell induced osteogenesis in porous hydroxyapatite and tricalcium phosphate. J. Biomed. Mater. Res. 24, 1563, 1990.
5. Ohgushi, H., Dohi, Y., Tamai, S., and Tabata, S. Osteogenic differentiation of marrow stromal stem cells in porous hydroxyapatite ceramics. J. Biomed. Mater. Res. 27, 1401, 1993.
6. Ohgushi, H., Yoshikawa, T., Nakajima, H., Tamai, S., Dohi, Y., and Okunaga, K. Al_2O_3 doped apatite-wollastonite containing glass ceramic provokes osteogenic differentiation of marrow stromal stem cells. J. Biomed. Mat. Res. 44, 381, 1999.
7. Ohgushi, H., and Caplan, A.I. Stem cell technology and bioceramics: From cell to gene engineering. J. Biomed. Mater. Res. 48, 913, 1999.

8. Kitamura, S., Ohgushi, H., Hirose, M., Funaoka, H., Takakura, Y., and Ito, H. Osteogenic differentiation of human bone marrow-derived mesenchymal cells cultured on alumina ceramics. Artif. Organs **28**, 72, 2004.
9. Ohgushi, H., Ikeuchi, M., Tateishi, T., Tohma, Y., Tanaka, T., and Takakura, T. Marrow mesenchymal stem cells cultured on alumina ceramics (from basic science to clinical application). Key Eng. Mater. **240**, 651, 2003.
10. Makino, S., Fukuda, K., Miyoshi, S., Konisho, F., Kodama, H., Pan, J., Sano, M., Takahashi, T., Hori, S., Abe, H., Hata, J., Umezawa, A., and Ogawa, S. Cardiomyocytes can be generated from marrow stromal cells *in vitro*. J. Clin. Invest. **103**, 697, 1999.
11. Reyes, M., Dudek, A., Jahagirdar, B., Koodie, L., Marker, P.H., and Verfaillie, C.M. Origin of endothelial progenitors in human postnatal bone marrow. J. Clin. Invest. **109**, 337, 2002.
12. Akahane, M., Ohgushi, H., Kuriyama, S., Akahane, T., and Takakura, Y. Hydroxyapatite ceramics as a carrier of gene-transduced bone marrow cells. J. Orthop. Sci. **7**, 677, 2002.
13. Schwartz, R.E., Reyes, M., Koodie, L., Jiang, Y., Blackstad, M., Lund, T., Lenvik, T., Johnson, S., Hu, W.S., and Verfaillie, C.M. Multipotent adult progenitor cells from bone marrow differentiate into functional hepatocyte-like cells. J. Clin. Invest. **109**, 1291, 2002.
14. Deng, W., Obrocka, M., Fischer, I., and Prockop, D.J. *In vitro* differentiation of human marrow stromal cells into early progenitors of neural cells by conditions that increase intracellular cyclic AMP. Biochem. Biophys. Res. Commun. **282**, 48, 2000.
15. Pittenger, M.F., Mackay, A.M., Beck, S.C., Jaiswal, R.K., Douglas, R., Mosca, J.D., Moorman, M.A., Simonetti, D.W., Craig, S., and Marshak, D.R. Multilineage potential of adult human mesenchymal stem cells. Science **284**, 143, 1999.
16. Jiang, Y., Jahagirdar, B.N., Reinhardt, R.L., Schwartz, R.E., Keene, C.D., Ortiz-Gonzalez, X.R., Reyes, M., Lenvik, T., Lund, T., Blackstad, M., Du, J., Aldrich, S., Lisberg, A., Low, W.C., Largaespada, D.A., and Verfaillie, C.M. Pluripotency of mesenchymal stem cells derived from adult marrow. Nature **418**, 41, 2002.
17. Spurr, E.E., Wiggins, N.E., Marsden, K.A., Lowenthal, R.M., and Ragg, S.J. Cryopreserved human haematopoietic stem cells retain engraftment potential after extended (5–14 years) cryostorage. Cryobiology **44**, 210, 2002.
18. Bruder, S.P., Jaiswal, N., and Haynesworth, E. Growth kinetics, self-renewal, and the osteogenic potential of purified human mesenchymal stem cells during extensive subcultivation and following cryopreservation. J. Cell. Biochem. **64**, 278, 1997.
19. Hirose, M., Kotobuki, N., Machida, H., Kitamura, S., Ohgushi, H., and Tateishi, T. Osteogenic potential of cryopreserved human bone marrow-derived mesenchymal cells after thawing in culture. Mater. Sci. Eng. C **24**, 355, 2004.
20. Kotobuki, N., Hirose, M., Takakura, Y., and Ohgushi, H. Autologous cultured human cells for hard tissue regeneration: Preparation and characterization of mesenchymal stem cells from bone marrow. Artif. Organs **28**, 33, 2004.
21. Reddi, A.H., and Sullivan, N.E. Matrix-induced endochondral bone differentiation: Influence of hypophysectomy, growth hormone, and thyroid-stimulating hormone. Endocrinology **107**, 1291, 1980.
22. Ikeuchi, M., Dohi, Y., Horiuchi, K., Ohgushi, H., Noshi, T., Yoshikawa, T., Yamamoto, K., and Sugimura, M. Recombinant human bone morphogenetic protein-2 promotes osteogenesis within atelopeptide type I collagen solution by combination with rat cultured marrow cells. J. Biomed. Mater. Res. **60**, 61, 2002.
23. Uchimura, E., Machida, H., Kotobuki, N., Kihara, T., Kitamura, S., Ikeuchi, M., Hirose, M., Miyake, J., and Ohgushi, H. *In situ* visualization and quantification of mineralization process of cultured osteogenetic cell. Calcif. Tissue Int. **73**, 575, 2003.
24. Hirose, M., Kotobuki, N., Machida, H., Uchimura, E., and Ohgushi, H. Quantitative monitoring of *in vitro* mineralization process using fluorescent dyes. Key Eng. Mater. **240**, 715, 2003.
25. Young, I.T. Proof without prejudice: Use of the Kolmogorov–Smirnov test for the analysis of histograms from flow systems and other sources. J. Histochem. Cytochem. **25**, 935, 1977.
26. Reyes, M., Lund, T., Lenvik, T., Aguiar, D., Koodie, L., and Verfaillie, C.M. Purification and *ex vivo* expansion of postnatal human marrow mesodermal progenitor cells. Blood **98**, 2615, 2001.
27. Colter, D.C., Sekiya, I., and Prockop, D.J. Identification of a subpopulation of rapidly self-renewing and multipotential adult stem cells in colonies of human marrow stromal cells. Proc. Natl. Acad. Sci. U.S.A. **98**, 7841, 2001.
28. Bianco, P., Riminucci, M., Gronthos, S., and Robey, P.G. Bone marrow stromal stem cells: Nature, biology, and potential applications. Stem Cells **19**, 180, 2001.
29. Majumdar, M.K., Thiede, M.A., Haynesworth, S.E., Bruder, S.P., and Gerson, S.L. Human marrow-derived mesenchymal stem cells (MSCs) express hematopoietic cytokines and support long-term hematopoiesis when differentiated toward stromal and osteogenic lineages. J. Hematother. Stem Cell Res. **9**, 841, 2000.
30. Mosca, J.D., Hendricks, J.K., Buyaner, D., Davis-Sproul, J., Chuang, L.C., Majumdar, M.K., Chopra, R., Barry, F., Murphy, M., Thiede, M.A., Junker, U., Rigg, R.J., Forestell, S.P., Bohnlein, E., Storb, R., and Sandmaier, B.M. Mesenchymal stem cells as vehicles for gene delivery. Clin. Orthop. **379**, 71, 2000.
31. Cheng, L., Qasba, P., Vanguri, P., and Thiede, M.A. Human mesenchymal stem cells support megakaryocyte and pro-platelet formation from $CD34^+$ hematopoietic progenitor cells. J. Cell. Physiol. **184**, 58, 2000.
32. Majumdar, M.K., Thiede, M.A., Mosca, J.D., Moorman, M., and Gerson, S.L. Phenotypic and functional comparison of cultures of marrow-derived mesenchymal stem cells (MSCs) and stromal cells. J. Cell. Physiol. **176**, 57, 1998.
33. Caplan, A.I., Reuben, D., and Haynesworth, S.E. Cell-based tissue engineering therapies: The influence of whole body physiology. Adv. Drug Deliv. Rev. **33**, 3, 1998.
34. Caplan, A.I. Mesenchymal stem cells. J. Orthop. Res. **9**, 641, 1991.
35. Chu, Q., Wang, Y., Fu, X., and Zhang, S. Mechanism of *in vitro* differentiation of bone marrow stromal cells into

neuron-like cells. J. Huazhong Univ. Sci. Technol. Med. Sci. 24, 259, 2004.
36. Young, D.A., Gavrilov, S., Pennington, C.J., Nuttall, R.K., Edwards, D.R., Kitsis, R.N., and Clark, I.M. Expression of metalloproteinases and inhibitors in the differentiation of P19CL6 cells into cardiac myocytes. Biochem. Biophys. Res. Commun. 24, 759, 2004.
37. Buchanan, S.S., Gross, S.A., Acker, J.P., Toner, M., Carpenter, J.F., and Pyatt, D.W. Cryopreservation of stem cells using trehalose: Evaluation of the method using a human hematopoietic cell line. Stem Cells Dev. 13, 295, 2004.

Address reprint requests to:
Hajime Ohgushi, M.D.
Research Institute for Cell Engineering
National Institute of Advanced Industrial Science and Technology
3-11-46 Nakoji
Amagasaki, Hyogo 661-0974, Japan

E-mail: hajime-ohgushi@aist.go.jp

Adrenomedullin Regenerates Alveoli and Vasculature in Elastase-induced Pulmonary Emphysema in Mice

Shinsuke Murakami, Noritoshi Nagaya, Takefumi Itoh, Takashi Iwase, Toshiya Fujisato, Keisuke Nishioka, Kaoru Hamada, Kenji Kangawa, and Hiroshi Kimura

Departments of Regenerative Medicine and Tissue Engineering, Biochemistry, and Internal Medicine, National Cardiovascular Center Research Institute, Osaka; Second Department of Internal Medicine, Nara Medical University, Nara; and Department of Transfusion Medicine, Hyogo College of Medicine, Hyogo, Japan

Rationale: Adrenomedullin, a potent vasodilator peptide, regulates cell growth and survival. However, whether adrenomedullin contributes to lung regeneration remains unknown. *Objectives:* To investigate whether adrenomedullin influences the kinetics of bone marrow cells, and whether adrenomedullin promotes regeneration of alveoli and vasculature and thereby improves lung structure and function in elastase-induced emphysema in mice. *Methods:* Adrenomedullin or vehicle was randomly administered to C57BL/6 mice for 5 days. We counted the numbers of mononuclear cells and stem cell antigen-1–positive cells in circulating blood. After intratracheal injection of elastase or saline, mice were randomized to receive continuous infusion of adrenomedullin or vehicle for 14 days. Functional and histologic analyses were performed 28 days after treatment. *Results:* Twenty-eight days after elastase injection, destruction of the alveolar walls was observed. However, adrenomedullin infusion significantly inhibited the increase in lung volume, static lung compliance, and mean linear intercept in mice given elastase. Adrenomedullin increased the numbers of mononuclear cells and stem cell antigen-1–positive cells in circulating blood. Adrenomedullin significantly increased the number of bone marrow–derived cells incorporated into the elastase-treated lung. Some of these cells were positive for cytokeratin or von Willebrand factor. Infusion of adrenomedullin after the establishment of emphysema also had beneficial effects on lung structure and function. *In vitro,* addition of adrenomedullin attenuates elastase-induced cell death in alveolar epithelial cells and endothelial cells. *Conclusions:* Adrenomedullin improved elastase-induced emphysema at least in part through mobilization of bone marrow cells and the direct protective effects on alveolar epithelial cells and endothelial cells.

Keywords: bone marrow cells; differentiation; mobilization; regeneration

Pulmonary emphysema, a major cause of respiratory dysfunction and death worldwide, is defined as abnormal permanent enlargement of airspaces distal to terminal bronchioles (1–3). Because many mediators with overlapping actions are involved in pulmonary emphysema, there is no effective treatment that prevents the progression of this disease. Destruction of the alveolar walls, one of the pathologic changes in pulmonary emphysema, had been considered irreversible. However, recent studies have demonstrated that bone marrow cells are mobilized into the peripheral blood to be involved in regeneration of alveoli (4, 5). Thus lung regeneration by bone marrow cells may be desirable for the treatment of pulmonary emphysema.

Adrenomedullin (AM) is a potent vasodilator peptide that was originally isolated from human pheochromocytoma (6). Immunoreactive AM has subsequently been detected in a variety of tissues, including the lungs (7, 8). The AM receptor has been shown to be expressed strongly in the basal cells of the airway epithelium and type II pneumocytes, both of which are involved in epithelial regeneration of the lung (9). Recent studies have shown that AM activates the phosphatidylinositol 3-kinase (PI3K)/Akt-dependent pathway in vascular endothelial cells, which is considered to regulate multiple critical steps in cell growth (10–13). These findings raise the possibility that AM may play an important role in the regulation of pulmonary homeostasis. However, whether AM is involved in lung regeneration remains unknown.

Thus the purposes of the present study were to (*1*) investigate whether infusion of AM influences the kinetics of bone marrow cells, (*2*) investigate the direct effects of AM on alveolar epithelial cells and endothelial cells, and (*3*) examine whether AM promotes regeneration of alveoli and vasculature in the lung and thereby improves lung structure and function in elastase-induced emphysema in mice.

METHODS

Animal Model

We used 10-week-old female C57BL/6 mice. To investigate whether AM influences the kinetics of bone marrow cells, AM or saline was randomly administered to 48 mice. Transgenic mice (C57BL/6 background) that ubiquitously express green fluorescent protein (GFP) were provided by Prof. Masaru Okabe (Osaka University, Japan) (14). To assess the kinetics of bone marrow cells, 10 GFP-positive bone marrow chimeric mice were established. Four weeks after bone marrow transplantation, the chimeric mice were given intratracheal injection of porcine pancreatic elastase (200 units/kg; Sigma, St. Louis, MO). An additional 42 wild-type mice were used to examine whether AM improves lung structure and function in elastase-induced emphysema. Finally, 10 GFP-positive bone marrow chimeric mice and 42 wild-type mice were used to examine the effects of AM on established emphysema. All protocols were performed in accordance with the guidelines of the Animal Care Ethics Committee of the National Cardiovascular Center Research Institute.

AM Preparation and Administration

Recombinant human AM was obtained from Shionogi Co., Ltd., Osaka, Japan. The homogeneity of AM was confirmed by reverse-phase, high-performance liquid chromatography and amino acid analysis. Forty-two wild-type mice were randomly given intratracheal injection of either elastase or saline and assigned to receive continuous infusion of AM or vehicle. AM was administered by a subcutaneous osmotic minipump (Alzet minipumps #1002; Durect Corp., Cupertino, CA) with a delivery rate of 0.05 μg/kg/minute for 14 days. This protocol resulted in the creation of three groups: sham mice given vehicle (sham group, n =

(Received in original form September 26, 2004; accepted in final form June 3, 2005)

Supported by the Research Grant for Cardiovascular Disease (16C-6) from the Ministry of Health, Labor and Welfare, the Industrial Technology Research Grant Program in 2003 from the New Energy and Industrial Technology Development Organization (NEDO) of Japan, Health and Labor Sciences Research Grants-genome 005, and the Promotion of Fundamental Studies in Health Science of the Organization for Pharmaceutical Safety and Research (OPSR) of Japan.

Correspondence and requests for reprints should be addressed to Noritoshi Nagaya, M.D., Department of Regenerative Medicine and Tissue Engineering, National Cardiovascular Center Research Institute, 5-7-1 Fujishirodai, Suita, Osaka 565-8565, Japan. E-mail: nnagaya@ri.ncvc.go.jp

Am J Respir Crit Care Med Vol 172. pp 581–589, 2005
Originally Published in Press as DOI: 10.1164/rccm.200409-1280OC on June 9, 2005
Internet address: www.atsjournals.org

14), elastase mice given vehicle (vehicle group, n = 14), and elastase mice treated with AM (AM group, n = 14). Ten GFP-positive bone marrow chimeric mice were divided into two groups: elastase mice given vehicle and elastase mice treated with AM (n = 5 each).

To investigate the effects of AM on established emphysema, the mice were randomly given intratracheal injection of either elastase or saline according to a previously described protocol by Massaro and colleagues (15). Twenty-five days after elastase or saline injection, the mice received continuous infusion of AM or vehicle for 12 days (sham, vehicle, and AM groups, n = 14 each). These mice were evaluated on Day 37. In addition, 10 GFP-positive chimeric mice were investigated by a similar protocol to assess the kinetics of bone marrow cells.

Isolation of Mononuclear Cells and Flow Cytometric Analysis

AM (1, 2, or 5 μg in 100 μl saline) was randomly administered to C57BL/6 mice (n = 8 each) by intraperitoneal injection daily for 5 days. Control mice received 100 μl saline according to the same schedule (n = 8). In addition, AM or vehicle was administered to other mice (n = 8 each) by a subcutaneous osmotic minipump with a delivery rate of 0.05 μg/kg/minute for 5 days. Blood samples were obtained on Day 5 and mononuclear cells were separated using Histopaque-1083 (Sigma), as described previously (16). The mononuclear cells were counted manually and analyzed for the expression of stem cell antigen-1 (Sca-1)–fluorescein isothiocyanate (BD Pharmingen, San Diego, CA). Immunofluorescence-labeled cells were analyzed by quantitative flow cytometry with a FACSCalibur flow cytometer (BD Biosciences, Mountain View, CA). An isotype-identical antibody (BD Pharmingen) served as a control.

Bone Marrow Chimeric Mice

Bone marrow chimeric mice were created as described previously (17). In brief, wild-type recipient C57BL/6 mice were lethally irradiated (900 cGy) and transplanted with GFP mouse-derived bone marrow cells (3×10^6 cells/300 μl) via the tail vein. To quantify the reconstitution of mouse bone marrow, peripheral blood mononuclear cells and bone marrow cells were analyzed by flow cytometry 4 weeks after bone marrow transplantation.

Assessment of Bone Marrow Cell Homing and Differentiation

Cryosections were obtained from the lungs of GFP-positive chimeric mice 28 days after elastase injection. The number of GFP-positive cells in the alveolar walls was counted and expressed as the number per 100 alveoli. Alveolar epithelial cells were identified using a murine monoclonal antibody anti–cytokeratin 5 and 8 (Chemicon, Temecula, CA) and a goat Alexa fluor 633–conjugated antimouse antibody (Molecular Probes, Eugene, OR) (4). Vascular endothelial cells were identified using a rabbit polyclonal antibody raised against von Willebrand factor (vWF; Dako, Copenhagen, Denmark) and a goat Alexa fluor 633–conjugated antirabbit antibody (Molecular Probes). The numbers of GFP/cytokeratin double-positive cells and GFP/vWF double-positive cells were counted and expressed as the number per 100 alveoli. Histologic examinations were performed in a blinded fashion by three observers.

Morphologic and Functional Analyses

Twenty-eight days after elastase or saline injection, the mice were paralyzed and static lung compliance was measured using a computer-controlled small animal ventilator (flexiVent; Scireq, Montreal, PQ, Canada; n = 7 each). The lungs were removed and fixed at a constant transpulmonary pressure of 25 cm H_2O for 24 hours (n = 7 each). The lung volume was measured by the method of Scherle (18). The mean linear intercept, a morphometric parameter of emphysema, was calculated by light microscopy on 20 randomly selected fields as described previously (19). Morphologic examinations were performed in a blinded fashion by three observers.

Assessment of Vascular Density

Paraffin sections were obtained from the lungs (n = 7 each). To investigate whether AM induces angiogenesis in the elastase-treated lung, tissue sections were stained for vWF (20). The number of vWF-positive vessels per millimeter squared was counted in a blinded fashion by three observers.

Assessment of Cell Proliferation

Cryosections were obtained from the lungs of GFP-positive chimeric mice. To investigate whether AM promotes cell proliferation, tissue sections were stained for Ki-67, a marker for cell proliferation, using a rat antimouse Ki-67 antibody (Dako) and a goat Alexa fluor 633–conjugated anti-rat antibody (Molecular Probes). The number of Ki-67–positive cells per millimeter squared was counted in a blinded fashion by three observers.

In Vitro Study

A549 human alveolar type II epithelial cells (American Type Culture Collection, Rockville, MD) were cultured in F-12K medium (Invitrogen Corp., Carlsbad, CA) supplemented with 10% fetal calf serum (Invitrogen Corp.) and 1% penicillin-streptomycin (Invitrogen Corp.). Human umbilical vein endothelial cells (HUVEC) (Cambrex Corp., East Rutherford, NJ) were cultured in Medium 199 (Invitrogen Corp.) supplemented with 20% serum and 1% penicillin-streptomycin. To investigate whether AM attenuates elastase-induced cell death, cells were treated with elastase (0.3 units/ml) along with various concentrations of AM (10^{-10} to 10^{-7} M) (21). Twenty-four hours after elastase administration, cell number and DNA fragmentation were assessed. Cell number was assessed using a CellTiter 96 aqueous one solution cell proliferation assay kit (Promega, Madison, WI) according to the manufacturer's directions (n = 4 each). DNA fragmentation was detected by terminal deoxynucleotidyl transferase–mediated dUTP biotin nick-end labeling (TUNEL) assay with a commercially available kit (ApopTag; Chemicon). The cells were then mounted in medium containing 4′,6-diamidino-2-phenylindole. The ratio of TUNEL-positive cells to total cells was calculated by counting at least 300 cells/well (n = 4 each). Finally, 6 hours after elastase administration, caspase-3 activity was measured with a commercially available kit (Promega) according to the manufacturer's directions (n = 4 each).

Assessment of Nitric Oxide Release and Detection of Soluble Kit-Ligand

In vitro, murine bone marrow stromal cells were prepared, as reported previously (26). Bone marrow stromal cells were cultured in Dulbecco's modified Eagle medium (Invitrogen Corp.) supplemented with 10% serum and 1% penicillin-streptomycin. The cells were treated for 20 minutes with control buffer, AM, or AM plus wortmannin (5×10^{-8} M; Wako Pure Chemical Ind., Ltd., Osaka, Japan), a PI3K inhibitor. To estimate total amounts of nitric oxide (NO) released from bone marrow stromal cells, nitrite content in the culture medium were measured using 2,3-diaminonaphthalene kit (Dojindo Laboratories, Kumamoto, Japan; n = 6 each).

In vivo, 5 days after continuous infusion of AM (0.05 μg/kg/minute) or vehicle, murine bone marrow plasma was collected by flushing femurs and tibias with a total of 0.5 ml saline. After spinning, supernatants were analyzed for soluble kit-ligand, a key molecule for stem cell recruitment, expression by ELISA (R&D Systems, Minneapolis, MN; n = 8 each) (22).

Measurement of Vascular Endothelial Growth Factor

To investigate the effect of AM on endogenous production of vascular endothelial growth factor (VEGF) in the elastase-injected mice, serum VEGF concentration was measured using a mouse VEGF ELISA kit (R&D Systems; n = 7 each).

Statistical Analysis

Numeric values were expressed as mean ± SEM unless otherwise indicated. Comparisons were made by one-way analysis of variance, followed by Newman-Keuls' test. A value of $p < 0.05$ was considered statistically significant.

RESULTS

Mobilization of Bone Marrow Cells

Administration of AM dose-dependently increased the number of peripheral blood mononuclear cells on Day 5 (Figure 1A).

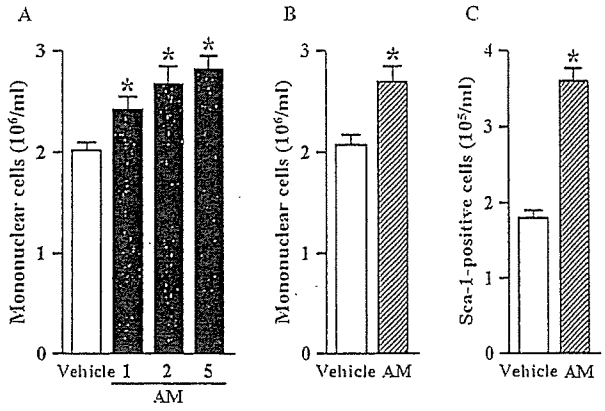

Figure 1. (*A*) Effect of bolus injection of adrenomedullin (AM) on the number of peripheral blood mononuclear cells. (*B*) Effect of continuous administration of AM on the number of peripheral blood mononuclear cells. (*C*) Effect of continuous administration of AM on the number of stem cell antigen-1 (Sca-1)–positive cells. Data are mean ± SEM. *White bars* = vehicle; *black bars* = bolus injection of AM (μg); *striped bars* = continuous administration of AM (0.05 μg/kg/minute). *$p < 0.05$ versus vehicle group.

A significant change was detected from the lowest dose (1 μg/mouse: 120% of vehicle group) to the highest dose (5 μg/mouse: 140% of vehicle group). A significant increase was also detected in mice administered AM by an osmotic minipump (131% of vehicle group; Figure 1B). Furthermore, the frequency of Sca-1–positive cells was significantly increased (200% of vehicle group; Figure 1C).

Regeneration of Pulmonary Epithelium

In the chimeric mice, the proportions of GFP-positive peripheral blood mononuclear cells and bone marrow cells were 87 to 93% and 85 to 90%, respectively, indicating that most of the original stem cell population was replaced by donor cells. Twenty-eight days after elastase injection, GFP-positive cells were detected in the alveolar walls. GFP/cytokeratin double-positive cells were also observed in the alveolar walls (Figure 2A). Semiquantitative analysis demonstrated that the number of GFP-positive cells incorporated into the lung was significantly increased in the AM group compared with that in the vehicle group (Figure 2B). In addition, the number of GFP/cytokeratin double-positive cells was significantly increased in the AM group compared with that in the vehicle group (Figure 2C). Twenty-eight days after elastase injection, the development of airspace enlargement with destruction of the alveolar walls was observed in the vehicle group (Figure 3A). However, administration of AM attenuated the histologic changes in mice given elastase. The mean linear intercept in the vehicle group was significantly increased compared with that in the sham group (Figure 3B), but the increase was significantly attenuated by AM.

Regeneration of Pulmonary Vasculature

GFP/vWF double-positive cells were observed in the alveolar walls (Figure 4A), and the number of these cells in the AM group was larger than that in the vehicle group (Figure 4B). As a whole, the number of vWF-positive pulmonary vessels was decreased 28 days after elastase injection (Figures 4C and 4D). However, AM infusion significantly increased the number of vWF-positive pulmonary vessels in the elastase-treated lung.

Effect of AM on Pulmonary Function

Twenty-eight days after elastase injection, the lung volume was significantly increased in the vehicle group (Figure 5A). The increase in lung volume was significantly attenuated by AM. Static lung compliance was significantly increased in the vehicle group, and the change was significantly attenuated by AM (Figure 5B).

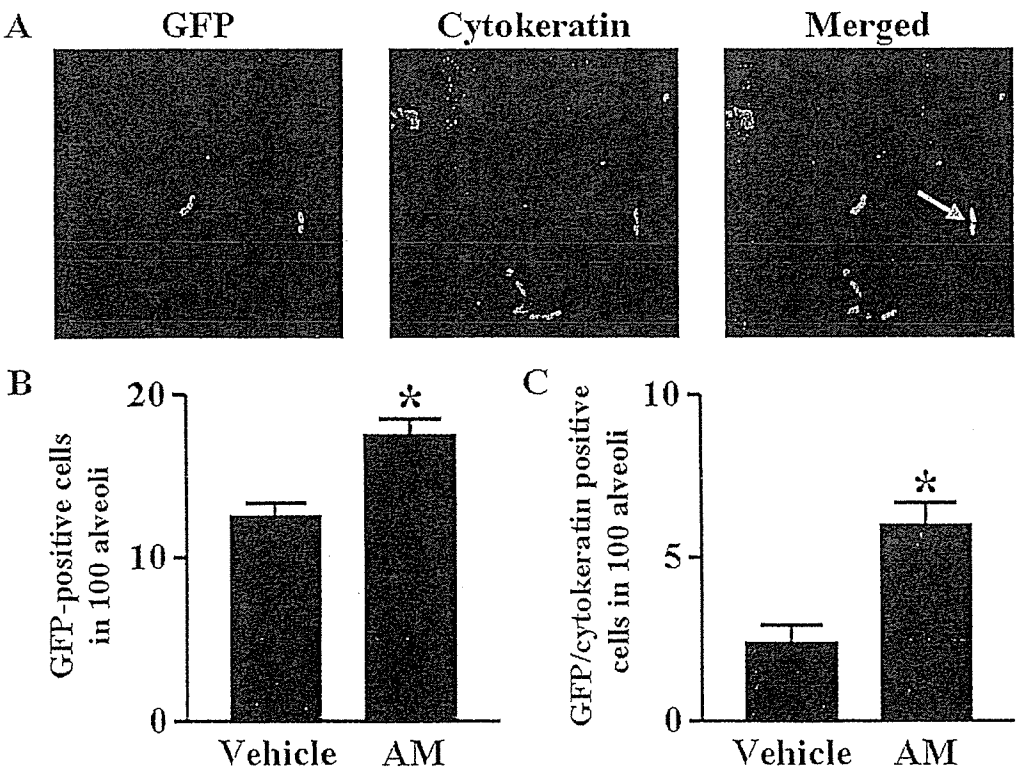

Figure 2. (*A*) Representative examples of bone marrow cell differentiation into epithelial lineage. Green fluorescence indicates green fluorescent protein (GFP); red fluorescence indicates cytokeratin, a marker for epithelial cells. Original magnification ×400. (*B*) Semiquantitative analysis of cell migration. The number of GFP-positive cells in the alveolar walls was significantly higher in the AM group than that in the vehicle group. (*C*) Semiquantitative analysis of epithelial differentiation. The number of GFP/cytokeratin double-positive cells was significantly higher in the AM group than that in the vehicle group. Data are mean ± SEM. *$p < 0.05$ versus vehicle group.